Retinal Vascular Reactivity to Incremental Hyperoxia During Isocapnia

by

Adrienne W. Tong

A thesis
presented to the University of Waterloo
in fulfillment of the
thesis requirement for the degree of
Master of Science
in
Vision Science

Waterloo, Ontario, Canada, 2008

AUTHOR'S DECLARATION

I hereby declare that I am the sole author of this thesis. This is a true copy of the thesis, including any required final revisions, as accepted by my examiners.

I understand that my thesis may be made electronically available to the public.

Abstract

Retinal Vascular Reactivity to Incremental Hyperoxia During Isocapnia

Purpose

Systemic hyperoxia has been induced using inspired gases in many studies to investigate vascular reactivity in the retinal vasculature. Technical limitations in the past resulted in inadequate control of systemic partial pressures of O_2 and CO_2, the latter of which tended to decrease secondary to induced hyperoxia. Recent development of a computerized gas delivery instrument has enabled the specific control of end-tidal CO_2 ($ETCO_2$) and fractional expired O_2 (FeO_2), independent of each other and of minute ventilation. The specific aims of each chapter are as follows:

Chapter 3: To compare the magnitude and variability of the retinal vascular reactivity response to an isocapnic hyperoxic stimulus delivered using a manually-operated method to the newly developed computer-controlled gas sequencer.

Chapter 4: To investigate the retinal hemodynamic response to incremental changes in hyperoxic stimuli during isocapnia.

Methods

Chapter 3: Ten young, healthy adults inhaled gases in a sequence of normoxic baseline, isocapnic hyperoxia, and normoxic recovery, using both gas delivery systems in random order.

Chapter 4: Twelve healthy, young adults participated in a gas protocol consisting of 4 phases at varying fractional expired oxygen levels (FeO_2): baseline (15%), hyperoxia I (40%), hyperoxia II (65%), and recovery (15%). End-tidal carbon dioxide ($ETCO_2$) was maintained at an isocapnic level (~ 5%) throughout the experiment.

In both Chapters 3 and 4, blood flow was derived from retinal arteriolar diameter and simultaneous

blood velocity measurements of the superior temporal arteriole, acquired at 1-minute intervals during each of the phases of the gas protocol.

Results

Chapter 3: There was no interaction effect between the phases and gas delivery methods ($p = 0.7718$), but $ETCO_2$ was significantly reduced during hyperoxia ($p = 0.0002$) for both methods. However, the magnitude of change in $ETCO_2$ was physiologically insignificant i.e. <1%. The two systems differed in terms of FeO_2 during hyperoxia, at a level of 85.27 ± 0.29% for the manual method, and 69.02 ± 2.84% for the computer method ($p < 0.05$). Despite this difference in oxygen concentrations, there was no difference in the vascular reactivity response for diameter ($p = 0.7756$), velocity ($p = 0.1176$), and flow ($p = 0.1885$) for equivalent gas phases between the two gas delivery systems. The inter-subject variability of retinal hemodynamic parameters was consistently lower using the computer-controlled gas sequencer.

Chapter 4: Repeated measures ANOVA showed that there were significant influences of incremental changes in FeO_2 on arteriolar diameter ($p < 0.0001$), blood velocity ($p < 0.0001$), and blood flow ($p < 0.0001$) in the retina. Paired t-tests of these retinal hemodynamic parameters during each phase in the gas sequence showed they were significantly different ($p < 0.05$) from each other, with the exception of baseline and recovery values. Incremental increases in FeO_2 caused a linear decrease in group mean arteriolar diameter ($R^2 = 1$, $p = 0.002$), group mean blood velocity ($R^2 = 0.9968$, $p = 0.04$), and group mean blood flow ($R^2 = 0.9982$, $p= 0.03$).

Conclusions

Chapter 3: Inter-subject variability for virtually all retinal hemodynamic parameters was reduced using the computer-controlled method, presumably due to a higher degree of gas control. However,

care needs to be exercised in the interprtetation of these results due to the relatively small sample size. A similar retinal hemodynamic response to isocapnic hyperoxia was induced using the two gas delivery systems, despite different levels of maximal FeO_2.

Chapter 4: Isocapnic hyperoxia elicits vasoconstriction and the reduction of retinal arteriolar blood flow in a dose-dependent manner over the range of FeO_2 explored in this study.

Acknowledgements

I would like to express my sincere gratitude to my supervisor, Dr. Christopher Hudson, for his mentorship, patience, and support throughout my graduate studies. I would also like to thank my thesis committee members Dr. John Flanagan and Dr. Natalie Hutchings for offering their unique perspectives and helpful advice on my thesis work.

A special acknowledgement goes to Dr. Joseph Fisher, Jay Han, and Alexandra Mardimae of the Toronto General Hospital for offering their technical expertise on the use of the computerized gas delivery system.

I would also like to acknowledge Erin Harvey for lending her invaluable assistance with statistical analysis.

I would also like to thank all of my colleagues of the Retina Research Group, especially Dr. Edward Gilmore, Jasleen Jhajj, Mila Kisilevsky, Dr. Patricia Rose, Faryan Tayyari, Subha Venkataraman, and Tien Wong for taking the time to help me especially at the early stages of my studies, and for being a great resource throughout my time here. I am honoured and privileged to have worked with such a talented group of individuals.

Thank you also to all the participants in the study for their selfless contributions to the understanding of retinal and respiratory physiology. Their patience and understanding have made my work much more enjoyable and their participation has greatly enriched my experiences as a graduate student.

Finally, I would like to thank my family and friends for their faith and encouragement throughout this endeavour. It was very important to me to have an excellent support network of people on whom I can always rely.

My graduate studies have been funded by the Canadian Institute of Health Research (CIHR), Ontario Graduate Scholarship (OGS), the University of Waterloo President's Graduate Scholarship, the University of Waterloo Graduate Scholarship, and the University of Waterloo School of Optometry Class of 1948 Scholarship.

Dedication

I dedicate this work to my parents, Ellen and Anthony Tong. You have worked hard over the years to provide me with all the things I needed to become the person that I am today. Thank you for allowing me to pursue my dreams, and for all the support and encouragement along the way.

Table of Contents

List of Figures

List of Tables

Chapter 1
Literature Review: The Physiology of Retinal Blood Flow

1.1 Anatomy and Physiology of Retinal Blood Flow

1.1.1 The Anatomy of Retinal Blood Supply

The blood supply to structures within the orbit arises from the ophthalmic artery, which originates from the internal carotid artery. Two separate blood supplies fulfill the nutritional and waste removal needs of the retina: these are the choroidal and retinal circulations, which are separated by the retinal pigment epithelial layer[1;2].

Arising from the ophthalmic artery within the orbit, the central retinal artery (CRA) supplies approximately the inner two-thirds of the retina. The CRA pierces the optic nerve approximately 10-15 mm behind the globe, running parallel with the central retinal vein within the optic nerve [1]. It passes through the lamina cribosa entering the optic disc just nasal to centre and branches superiorly and inferiorly. These branches divide into nasal and temporal branches, and continue to bifurcate within the retinal nerve fibre layer below the transparent internal limiting membrane to supply the quandrants of the retina [3].

The outer layers of the retina are supplied by the highly vascularized choroidal circulation, derived from the ophthalmic artery via branches of the long posterior ciliary artery, short posterior ciliary artery, and anterior ciliary artery. Specifically, the short posterior ciliary artery supplies the posterior choroid, while the long posterior ciliary artery and anterior ciliary artery supply the anterior choroid and the circle of the iris. It is composed of three vascular layers: the choriocapillaris lies internally, followed by Sattler's layer with medium-sized vessels, and Haller's layer with large veins. The anatomical border between the retina

and the choroid is Bruch's membrane [4]. Adjacent to Bruch's membrane, the retinal pigment epithelium acts as the blood-retina barrier and selectively transports nutrients and waste between the choriocapillaris and the neural retina due to its avascular nature[5]. The retinal capillaries, unlike those in other capillary beds in the body, consist of unfenestrated endothelial cells joined together by *zonulae occludentes* (tight junctions), further contributing to the blood-retina barrier. This prevents vascular leakage into the retina and is important for protecting it against infection and the potentially damaging effects the body's immune system. The blood retina barrier is compromised in diseases such as diabetic macular edema [6;7] and acquired immunodeficiency syndrome (AIDS) [8].

The choroidal circulation has many distinctions from the retinal circulation. Traditionally, it was thought that the choroidal circulation does not exhibit autoregulation whereas the retina is autoregulated [3]. However, more recent evidence would suggest that autoregulation does occur in the choroid, though not as efficiently as compared to the retina [9-11]. At 18 mL/min per gram of tissue, the choroid carries 85% of the blood flow volume in the eye, whereas the retina carries only 0.5 - 1.7 mL/min per gram of tissue due to relatively sparse distribution of retinal vessels [12;13]. A high blood flow rate in the choroid is thought to have a thermoregulatory function; blood flowing through the choroid dissipates the heat generated by phototransduction in the neural retina [12]. The high and low blood flow rates of the choroid and retina respectively leads to a low arteriovenous pO_2 difference (3%) in the choroid, and a larger arteriovenous pO_2 difference (38%) in the retina since oxygen extraction is proportional to the rate of blood flow; the fact that the retina is also the most metabolically active tissue in the body further contributes to the large arteriovenous pO_2 difference [3;12]. Furthermore, the terminal branches of the retinal arteries do not anastomose with other arteries, and are described as end-arterial in nature. Consequently, the inner retina has a low capacity to tolerate interruption to the blood supply[14], making retinal blood flow an important

area of research [2;15]. Disruption of retinal blood flow has been implicated in sight-threatening conditions including glaucoma [16;17] and diabetic retinopathy [18-21].

Blood leaves the retina through the central retinal vein, which lies with the central retinal artery. Like other tributaries of the ophthalmic veins, the central retinal vein has no valves so blood flow is determined by pressure gradients. The central retinal vein either joins the superior ophthalmic vein or drains directly into the cavernous sinus. The choroid is drained via the vortex veins [22].

1.1.2 Structure of Retinal Vessels

The retinal vasculature is highly specialized in maintaining local control of blood flow. Histologically, retinal capillaries are composed of a single layer of unfenestrated, non-porous endothelium surrounded by an interrupted layer of pericytes, and a basement membrane. Tight junctions between the endothelial cells prevent vascular leakage into the neural retina (as described in 1.1.1). The retinal arterioles and venules are also composed of three layers, but a smooth muscle layer is present in place of the pericytes [23]. While venules have only a single or double layer of smooth muscles, the number of smooth muscle layers found in arterioles is proportional to the vessel calibre, ranging from a few to more than 10 layers. Smooth muscle cells in the arteriolar wall are the primary contractile elements that regulate blood flow to maintain retinal perfusion and, to a lesser extent, pericytes in the capillary wall further "fine tune" local flow. Both smooth muscle cells and pericytes facilitate blood flow through their contractile function in response to vascular endothelium-derived mediators and other metabolites[12]. As with other vascular beds within the body, the arterioles are "resistance vessels" through which blood is released into the capillaries, which mediate exchange of gases, nutrients, and wastes with the tissue "exchange vessels".

1.2 Blood Flow

1.2.1 Ohm's Law

Blood flow is the quantity of blood flowing through a given segment of a blood vessel in the general circulation in a given period of time. Blood flow (Q) through a vessel is determined by a pressure gradient (ΔP) and vascular resistance (R). The pressure gradient is the pressure difference between the two ends of the vessel, this is the force that propels the blood. Vascular resistance is the force opposing the pressure gradient as a result of friction of the vessel wall. These two factors are related by Ohm's Law.

$$Q = \frac{\Delta P}{R} \tag{1.1}$$

1.2.2 Vascular Resistance

Assuming that blood flow is steady and that the vessel is a rigid cylindrical tube, vascular resistance (R) is proportional to the viscosity of the blood (η) and the length of vessel (L), and inversely proportional to the fourth power of the radius of the vessel (r). The relationship of these factors to vascular resistance is summed up by the following equation:

$$R = \frac{8\eta L}{\pi r^4} \tag{1.2}$$

Since vascular resistance is inversely proportional to the fourth power of the radius, it is clear from this equation that vessel diameter has the greatest influence of all the factors combined. As such, change in vessel diameter plays an important role in the regulation of blood flow. The factors mediating vasoconstriction and vasodilation will be discussed in later sections.

1.2.3 Poiseuille's Law of Laminar Blood Flow

Laminar flow (or streamline, non-turbulent flow) occurs when fluid flows in parallel layers in a concentric arrangement within a cylindrical tube, without disruption between the layers. During laminar

flow, a parabolic velocity profile is formed since fluid molecules adhering to the vascular endothelium in the outermost lamina move the slowest, while adjacent layers move with increasing velocity towards to the centre (Figure 1-1). Poiseuille's law integrates the velocities of all the concentric rings of the velocity profile. It combines Ohm's Law and the factors affecting vascular resistance for the following equation:

$$Q = \frac{\pi \Delta \mathrm{Pr}^4}{8\eta L} \tag{1.3}$$

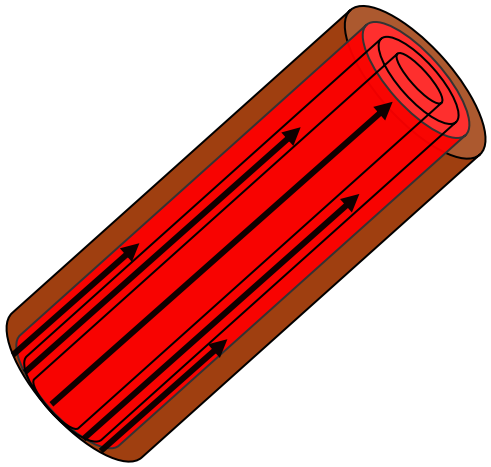

Figure 1-1. Poiseuille's Laminar Flow.
Concentric layers of fluid (blood) flow through this segment of blood vessel. The black arrows represent the velocity of blood flowing through each layer, with increasing velocity toward the centre.

There are some limitations to the application of Poiseuille's law *in vivo* due to several potentially flawed assumptions. Contrary to the assumption of Poiseuille's model, blood is a non-Newtonian fluid since viscosity can be altered by hematocrit, fibrinogen level, erythrocyte flexibility, and temperature [24;25] . Furthermore, blood vessels are elastic, such that an increased arterial pressure increase not only increases the perfusion pressure, but also distends the vessel and changes vascular resistance [26]. However, it is still generally accepted as an adequate approximation of blood flow *in vivo*. Poiseuille's law generally applies in relatively straight segments of the blood vessel, although turbulent flow occurs in curved segments, where there is branching, or in large blood vessels (eg. the aorta).

1.2.4 Retinal Blood Flow

As discussed in section 1.2.1, blood flow through a vessel is dependent on a pressure gradient and resistance to flow. The pressure gradient, or perfusion pressure, is defined as the difference between local arterial pressure (P_a) and local venous pressure. Venous pressure is assumed to be equal to intraocular pressure (IOP) for retinal blood flow [27]. Blood flow in the retinal vessels is consistent with Poiseuille's law of laminar flow [28].

Intraocular Pressure

Intraocular pressure (IOP) is the tissue pressure of the ocular contents. This pressure generated by the forces exerted by the aqueous produced at the ciliary processes, which flows through the posterior chamber and into the anterior chamber, and drains through the Canal of Schlemm and the episcleral veins. Clinically, IOP can be measured using applanation tonometry. The normal range for IOP is 10-22 mmHg, a range which ensures an adequate perfusion in the eye.

Blood Pressure

Blood pressure is a result of the force exerted by blood as it pumped by the heart throughout the vasculature. In the systemic circulation, blood pressure normally ranges between 120 mmHg during systole and 80 mmHg during diastole. Clinically, blood pressure can be measured using a sphygmomanometer.

Mean arterial pressure (MAP) is the average blood pressure over a single cardiac cycle. It is considered the perfusion pressure of the vascular beds throughout the body. When diastolic pressure (DP) and systolic pressure (SP) are known, it can be approximated by the following formula:

$$MAP = \frac{1}{3} DP + \frac{2}{3} SP \tag{1.4}$$

Ocular Perfusion Pressure

Ocular perfusion pressure (OPP) is the pressure of blood in the ocular tissues, which sets up the gradient for flow. Ocular perfusion pressure is related to mean arterial pressure (MAP) and intraocular pressure (IOP). It is calculated as follows:

$$OPP = \frac{2}{3} MAP - IOP \tag{1.5}$$

Conditions that increase OPP beyond the limits of autoregulatory capacity of the retinal vessels have the effect of increasing blood flow to the retina. Exercise-induced increase in MAP and decreased IOP result in an increased rate of blood flow in the choroid as a result of increase in OPP[9;10] and less efficient autoregulation of the choroid, whereas no such change in blood flow occurs within the inner retinal circulation . Ocular perfusion pressure also varies diurnally, with postural changes, and increases with age[29;30]. Regulation of blood flow in the face of changes in OPP due to postural change demonstrates

pressure autoregulation, which will be further discussed in section 1.3.1. Dysregulation of this response is associated with the pathogenesis of glaucoma[31] and diabetic retinopathy[18;19].

1.3 Regulation of Retinal Blood Flow

Blood flow to the retina is determined by the perfusion pressure and the diameter of the resistance vessels (arterioles). Unlike the choroidal and retrobulbar circulation which display autonomic nervous system control, the retinal vasculature lacks sympathetic fibres[13], and as such there is no nervous system control contribution to retinal vascular resistance. The retinal and optic nerve head vessels have α-adrenergic, β-adrenergic, and cholinergic receptors, but the role of these is unclear[32]. Local metabolic and myogenic stimuli, vascular endothelium-derived substances, and oxygen and carbon dioxide tension are major modifiers in vessel diameter, which is a major determinant of blood flow to the tissue since retinal arterioles lack precapillary sphincters, which play a role in regulating blood flow in other capillary beds[13].

Autoregulation in the retinal vasculature ensures that adequate perfusion of tissue in the face of changing nutrient requirements proportional to metabolic activity and alterations in perfusion pressure. Autoregulation normally refers to the maintenance of constant blood flow in the face of changes in OPP. Metabolic autoregulation refers to change in blood flow as a result of changing nutrient supply, including O_2 and CO_2. Various types of autoregulation and the factors mediating this response in the retina will be reviewed in the following sections.

1.3.1 Pressure Autoregulation

Pressure autoregulation is defined as the ability of the tissue to maintain relatively constant blood flow in the face of changes in perfusion pressure. This type of autoregulation only occurs within certain limits. In

the human retina, the upper limit for IOP for autoregulation is approximately 50 mmHg (corresponding to a mean retinal perfusion pressure of 10 mmHg), although it is only fully effective if mean retinal perfusion pressure is reduced by less than 50% (ie. IOP does not surpass 27-30 mmHg)[33]. A minimum IOP of 6 to 7 mmHg is also required[34]. Increments in brachial MAP, a measure of systemic blood pressure, correspond to change in ophthalmic artery pressure. As systemic blood pressure rises above approximately 40% from baseline values (ie. brachial MAP is 115 mmHg), the human retina fails to regulate flow against changes in retinal perfusion pressure[35]. Pressure autoregulation in response to change in systemic MAP has been studied under conditions of exercise[35-37], postural change[31], and systemic hypertension[38].

1.3.2 Myogenic Mechanism

Transmural pressure is the pressure difference between the lumen and the outside of a blood vessel, in contrast to perfusion pressure, which is the pressure difference between two different points within a vessel. The myogenic mechanism of autoregulation is related to the Bayliss Effect, which describes the contractile reaction of smooth muscle cells in arteriole walls due to an increase in transmural pressure[37]. Perfusion pressure varies during the cardiac cycle and is sustained by changes in MAP; this changes intraluminal pressure as blood flows through. When increased intraluminal pressure induces stretching in the lumen of the vessel, voltage-gated calcium channels are involved in the reactive constriction of the smooth muscle cells in retinal arterioles[39]. Endothelial cells lay at the interface between blood and the smooth muscle layer the blood vessels. Shear stress is the force acting tangentially on the endothelial cells in the direction of blood flow. The microvilli located on the apical surface of endothelial cells detects the hydrodynamic force exerted by shear stress and causes rearrangement the actin filaments in the cytoskeleton to and deformation of the cells[40]. This triggers the release of nitric oxide (NO), a potent

vasodilator[26;41]. The lack of sympathetic innervation of retinal vessels makes the intrinsic contractility of vascular smooth muscle cells an important factor in the regulation of retinal blood flow.

1.3.3 Metabolic Autoregulation/Vascular Reactivity

Metabolic autoregulation is the ability of a tissue to alter perfusion pressure to match tissue O_2, CO_2 and nutrient needs[42]. Metabolism in the neural retina is largely affected by light stimulation. Flickering light enhances glucose consumption; however, constant light reduces metabolism while the onset of light causes a spurt in metabolism[43]. Flicker stimulation increases blood flow to the optic nerve head and the retina[44;45] to support increased nutrient requirements, particularly in the perifoveolar region where ganglion cells and nerve fibres are concentrated[46]. Flicker-induced hyperemia is a result of vasodilation of retinal arteries[45;47] due to enhanced NO production under these conditions[48]. In contrast, choroidal blood flow is unaffected by flicker stimulation[49] despite the hypothesis that oxygen from the choroid is required to support the metabolic activity of the retina[50]. However, a blue flicker stimulus elicits an increase in subfoveal choroidal blood flow, perhaps in response to stimulation of colour-sensitive cones in the fovea[51]. This evidence suggests that metabolic autoregulation in the retina and choroid depends on regional sensitivity to stimulation at different wavelengths of light due to the distribution of rods and cones.

The high metabolic activity in the neural retina necessitates a steady supply of oxygen since aerobic cellular respiration releases more energy from glucose, than anaerobic glycolysis. In the presence of a flicker stimulus, there is an increase in retinal arteriovenous pO_2 difference since arterial and capillary pO_2 increases while no change in venous pO_2 is observed, indicating the increased oxygen extraction[52]. However, in agreement with the finding that flicker stimulus does not affect choroidal blood flow[49], the same phenomenon is not observed in the choroid[52].

Systemic changes in pO_2 and pCO_2 also require autoregulation at the level of the retina. Systemic hyperoxia (increased arterial pO_2) elicits retinal vasoconstriction[53] resulting in a decrease in blood flow to the retina[54-56]. An intact vascular endothelium is essential for this response since it is mediated by a potent vasoconstrictor, endothelin-1 (ET-1)[57;58]. When arterial pO_2 is increased, O_2 is delivered from the choroid to the deep retinal capillaries, and almost the whole thickness of the retina can be adequately supplied by the choroid alone[59]. Hypoxia (decreased pO_2) stimulates the release of another endothelium-derived factor, nitric oxide (NO), which causes vasodilation in the retinal vessels to increase capillary perfusion[60;61] while also enhancing the uptake of oxygen in local tissues[62]. Regulation of pO_2 in the retina is important to avoid ischemia if underperfused, or in the opposite situation, to avoid the potentially damaging effects of reactive oxygen species in hyperoxia[63]. Oxidative stress is linked to the pathogenesis of age-related macular degeneration[64], and retinopathy of prematurity[65].

Carbon dioxide causes vasodilation and an increase in blood flow in the retinal[66] and choroidal circulations[67;68]. The retina is very sensitive to changes in systemic pCO_2: a 1% rise in arterial pCO_2 can induce a 3% rise in blood flow. Although changes in arterial pCO_2 and pH of the interstitial retina are closely related, acidification of blood by lactate injection does not affect interstitial pH or retinal blood flow. Furthermore, systemic hypoxia induces an increase in retinal lactate release, which potentially affects vascular tone, as demonstrated by pre-retinal microinjections of lactate. Together, this suggests that interstitial – rather than systemic – acidosis is a requirement for a retinal vasomotor response to hypoxia[3]. Lactate is produced both aerobically and anaerobically with glucose consumption in the retina[69]. Oxidation of glucose into CO_2 in the retina thus affects vasomotor tone in the retinal vasculature. Carbogen studies further demonstrate the impact of pCO_2 on retinal metabolic autoregulation. When carbogen (a gas mixture of 95% O_2 and 5% CO_2) is inspired, it is thought to relatively improve retinal

oxygenation since it results in a less pronounced vasoconstriction than when 100% oxygen is delivered, allowing blood through the retinal vasculature at a higher rate[70]. Although inspiring 100% O_2 enhances oxygenation of the retina in the treatment of central retinal artery occlusion, co-administration of CO_2 would prevent ischemia due to decreased perfusion pressure.

The purest definition of "autoregulation" implies change in transmural pressure. However, transmural pressure is not a factor in the initiation of "metabolic autoregulation". For this reason, many authors use the term "vascular reactivity" rather than metabolic autoregulation. The term vascular reactivity will be utilized in this thesis from this point forward.

1.3.4 Endothelium-Derived Factors Affecting Vascular Tone

Nitric oxide (NO) is synthesized by three distinct isoforms of the enzyme nitric oxide synthase, but the isoform that is pertinent to vascular tone is endothelial nitric oxide synthase (eNOS). Endothelial cell-derived NO diffuses into smooth muscle cells and pericytes causing a change of biochemical events leading to vasodilation[1]. Due to the very short half-life of NO[71], production is controlled at the level of biosynthesis[41]. eNOS catalyzes the oxidation of L-arginine, which is then further oxidized to become NO, a potent vasodilator that is found systemically but also plays a crucial role in regulating ocular blood flow[41]. NO is continuously produced in the choroid, optic nerve head vessels, and retinal vessels and contributes to basal retinal vascular tone [72]. Flicker stimuli-induced vasodilation is mediated by NO[48;72;73], which is consistent with the observation that blood flow at the optic nerve head is proportional to neuronal activity [74;75]. This ensures adequate blood supply to support increased metabolic activity. Nitric oxide is also directly stimulated by, and in some cases important, in the vasomotor responses elicited by bradykinins, insulin-like growth factor-1, acetylcholine, thrombin, and various platelet products[1;41].

Endothelins (ET-1, ET-2, and ET-3) are another family of endothelium-derived vasoactive peptides (consisting of 21 amino acids each) that bind to adjacent pericytes and smooth muscle cells. They are currently the most potent known vasoconstrictor agents and their actions are mediated by three receptor subtypes (ETR-A, ETR-B, and ETR-C)[1]. Different isopeptides and receptors are located in a different set of organ systems, and function differently. Of the endothelin isopeptides, ET-1 is the one that is involved in modulating vasomotor tone via ETR-A[76]. Hyperoxia-induced vasoconstriction in the retina has been shown to be dependent on ET-1[57;58]. However, endothelins are also known to promote the release of vasodilators, prostacyclin and NO, making their net effect on a vascular bed difficult to predict[3]. The significance of this is unclear, although it could presumably be part of a feedback loop that maintains vascular tonus at the appropriate level.

1.4 The Measurement of Retinal Hemodynamics

The eye retinal vasculature is unique from other vascular beds in the body in that it can be viewed non-invasively. Many techniques have been developed to measure ocular blood flow in the retinal macro- and micro-circulations, choroid, and retrobulbar arteries to provide a concerted view of hemodynamics in different parts of the eye. Blood flow is classically described in millimeters per minute per gram of tissue which gives the most complete information about blood flow to metabolically active tissue. However, the currently available technologies do not report blood flow in these units. In some cases they are even reported in arbitrary units. As such, direct comparison of the results obtained using different procedures cannot be made. To date, the Canon Laser Blood Flowmeter is the only instrument that can assess retinal blood flow in absolute units. Nonetheless, each approach provides insight into how blood flow is affected by different stimuli and in healthy and diseased eyes. This section will describe some the techniques of retinal hemodynamic assessment.

1.4.1 Pulsatile Ocular Blood Flow

The measurement of pulsatile ocular blood flow (POBF) is based on the relationship between the observable pulsatile change in IOP during the cardiac cycle and the resulting change in the ocular volume. It is based on the principle that intraocular pressure increases as blood volume in the eye increases during systole[1]. POBF can be assessed using pneumotonometry or interferometry.

1.4.2 Pneumotonometry

The POBF instrument is a pneumotonometer that measures real-time IOP, recording changes in IOP during the cardiac cycle which exhibits a rhythmic sinusoidal pattern with a range of up to 2 mmHg[77]. The recorded IOP wave is converted into an ocular volume based on a presumed universal relationship but does not account for reflux and constant outflow[1;77]. Until recently, it was unclear which ocular vascular beds were being observed in POBF measurements. Zion et. al. combined this technique with colour Doppler imaging (1.4.9) and demonstrated that POBF was associated with the systolic and pulsatile components of blood velocity in both the temporal short posterior ciliary artery and the central retinal artery[78]. This result indicates that POBF have both choroidal and retinal components[78;79].

The measurement of POBF is considered an indirect hemodynamic indicator, since only IOP is measured. One of the major disadvantages of this technique is that the true volume of the blood bolus entering the eye during systole is unknown, since venous outflow and reflux are unknown [77]. Furthermore the use of the pneumotonometer significantly lowered IOP measurements[80], so the technique itself interferes with the outcome.

1.4.3 Laser Interferometry

Interferometry directly measures fundus pulsation relative to the cornea, but like pneumotonometry, remains an indirect measure of blood flow. Due to the relative strength of the sclera, when the choroid engorges with blood during systole, the fundus moves anteriorly towards the cornea, decreasing the distance separating them (optical length) [35;77]. A single laser beam passes through the eye and is partially reflected back by the cornea and the fundus. The interference pattern formed by the light reflected from these two sources changes in its geometry as the distance between the retina and the cornea varies with the cardiac cycle. The magnitude of the fundus pulsation can be calculated from the change in the interference pattern, which is measured by a linear array detector that quantifies the light level along its axis[1]. In the measurement of POBF, interferometry can measure fundus movement in micrometers although actual POBF is still unitless[1]. Laser interferometric measurements of POBF and pulse amplitude correlate well with measurements taken with a pneumotonometer and are considered a valid index of pulsatile choroidal perfusion in humans[79;81;82].

1.4.4 Fluorescein Angiography with Confocal Laser Ophthalmoscopy

Quantification of retinal blood flow using fluorescein angiography is based on the measurement of the amount of time it takes for fluorescein injected into a peripheral vein to appear and travel through the retinal vasculature. This technique yields several parameters including mean circulation time (MCT), arteriovenous passage (AVP) time, and mean dye velocity (MDV). The measurement of these parameters involves the use of dye dilution curves. The MDV is the time delay between dye arrival at two points in a vessel. The MCT (also referred to as mean transit time) is the average time that a fluorescein molecule spends in the retinal vascular bed. The AVP, which is used as an alternative for measuring MCT is defined as the time between the first appearance of dye in a retinal artery and corresponding retinal vein[83].

Angiographs of the fluorescein moving through the retinal vasculature was originally recorded as a series of photographs. Dye dilution curves were plotted based on the known concentration of the dye and the density (fluorescence intensity) as assessed from the photographs. This technique was limited by the frequency with which the photographs could be taken. Since the introduction of photographic quantitative angiography[84], recording of angiographs has been improved with the use of fluorophotometry[85], and fundus video cameras which provided a motion picture to increase enhanced the temporal resolution (sampling rate)[83].

Scanning laser ophthalmoscopy is the most current adaptation of this procedure. The Heidelberg retinal angiography (HRA) system has as a digital imaging device equipped with argon and near infrared lasers. The Rodenstock scanning laser ophthalmoscope (SLO), another imaging device, is equipped with argon, infrared, and helium-neon lasers. Both systems have a confocal optical system, whereby laser light reflected from the point interest in the fundus is focused through a confocal aperture and quantified by a photodetector after scattered light from adjacent sources are blocked by the confocal filter[1]. The current use of scanning laser ophthalmoscopes for fluorescence angiography provides spatial and temporal resolution that is superior to previous techniques[83]. This method is capable of measuring vessel diameter and is also sensitive to small temporal changes in retinal hemodynamics as well as regional differences in retinal blood flow. It remains, however, a relatively invasive technique of measuring retinal hemodynamics[1].

1.4.5 Laser Doppler Velocimetry

The Doppler effect is the change in frequency and wavelength of a wave as perceived by the observer that is moving relative to the source of the wave. This phenomenon is exploited by laser Doppler devices to measure the velocity of erythrocytes passing traveling through a blood vessel. A laser emitting light at a

known frequency (f) is directed at a blood vessel. The frequency of light scattered by a stationary source (ie. the vessel wall) is unaffected (f) while the frequency of light scattered a moving source (ie. the erythrocytes) is Doppler shifted (f") (Figure 1-2). The frequency of the shifted light is determined by the beat frequency (f"-f) caused by interference between shifted and non-shifted light.

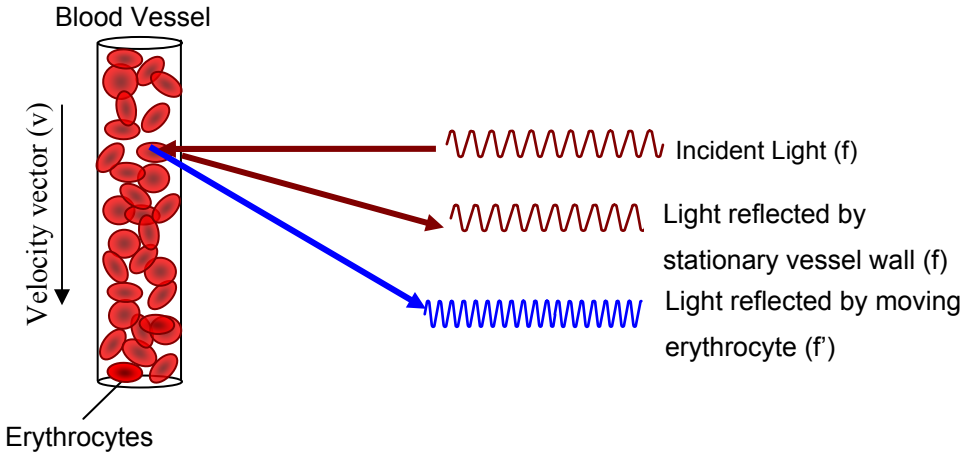

Figure 1-2. **Doppler Effect in Blood Vessels.**
The frequency laser light is Doppler-shifted if it is scattered by moving erythrocytes, but remain unaffected if scattered by surrounding tissue that is stationary.

The Doppler-shifted frequency of the light scattered by erythrocytes is proportional to the velocity of movement. The Doppler shift frequency spectrum (DSFS) recorded from blood column exhibits a cutoff frequency which is directly related to the maximum velocity[86]. The maximum velocity (v_{max}) is calculated from Doppler-shifted frequency (f_{max}) arising from the light scattered by the fastest-moving erythrocytes, while estimating the effects of the intraocular scattering geometry[87]. This relationship, where λ is the wavelength of the incident laser light, *n* is the index of the flowing medium, θ_i is the intraocular angle between the incident light and the velocity vector, and θ_s is the intraocular angle between the scattered light and the velocity vector is expressed below.

$$v_{max} = \frac{\lambda f_{max}}{n(\cos\theta_s - \cos\theta_i)} \tag{1.6}$$

Where Poiseuille's flow applies, the determination of maximum velocity or (v_{max}) – which corresponds to the centre of the blood column – is sufficient for calculating the volumetric flow rate (F). F is related to v_{max} by the following equation, where s is the cross-sectional area of the vessel at the measurement site[86].

$$F = \frac{1}{2} v_{max} s \tag{1.7}$$

1.4.6 Bidirectional Laser Velocimetry

By using a system of two photodetectors separated by a known angle, the absolute measurement of the speed of erythrocytes flowing through the retinal vessels was possible[87]. In bidirectional laser Doppler velocimetry, scattered laser light is measured in two directions characterized by wave vectors K_1 and K_2, while the direction of the incident laser is kept constant (Figure 1-3). The frequency shift is defined as the difference between the maximum frequencies associated with the wave vectors, since the frequency is shifted to different degrees when measured in different directions.

$$\Delta f = f_{2max} - f_{1max} = (\alpha_2 - \alpha_1)\frac{v}{\lambda} \tag{1.8}$$

where f_{1max} and f_{2max} are the cutoff frequencies associated with K_1 and K_2 respectively. The angles α_1 and α_2 are the angles separating the K_1 and K_2 vectors from the velocity vector, v.

The maximum velocity is obtained from the DSFS according to the following relationship

$$v_{max} = \frac{\lambda \Delta f}{n \Delta\alpha \cos\beta} \tag{1.9}$$

where λ is the wavelength of the incident laser beam, *n* is the index of refraction of the flowing medium, Δα is the angle between K_1 and K_2, and β is the angle between the velocity vector (v_{max}) and its projection on the plane defined by K_1 and K_2[88]. The use of two parallel photomultiplier tubes allows the unit to deduce the orientation of the blood vessel, and hence the direction of blood flow. This is important since the magnitude of the Doppler shift is dependent on the angle between the source (ie. the velocity vector) and the observer (the photomultiplier tubes)[1].

As an improvement from its precursor instruments, measurements made the bidirectional laser Doppler velocimeter are independent from ocular refraction. Furthermore, target fixation is done with the eye under examination rather than the fellow eye as in previous instruments, resulting in better stabilization of the retina for measurements[88].

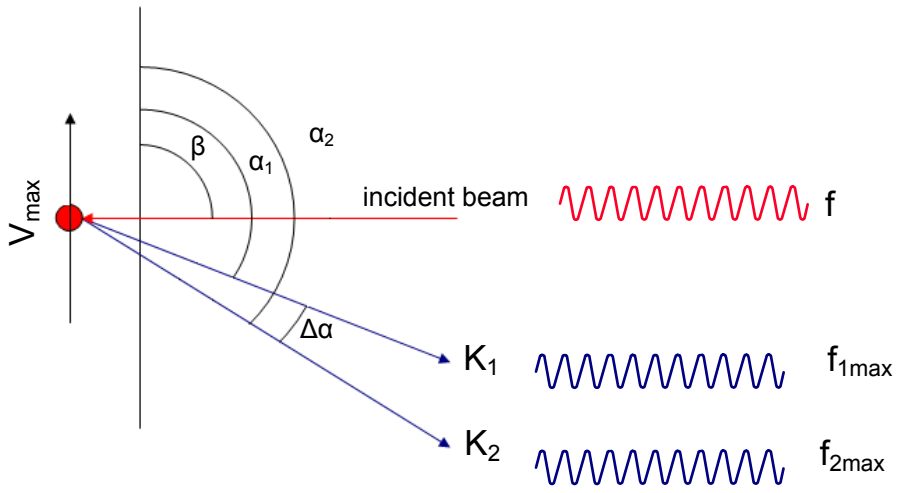

Figure 1-3. Bidirectional Laser Doppler Velocimetry.
v_{max} is the velocity vector of red blood cell, f is frequency of incident laser beam, f_{1max} and f_{2max} are the cutoff frequencies associated with the reflected beams K_1 and K_2 respectively, α_1 and α_2 are the angles

separating K_1 and K_2 from v_{max}, $\Delta\alpha$ is the angle that subtends K_1 and K_2, and β is the angle between v_{max} and its projection on the plane defined by K_1 and K_2. (Diagram courtesy of C. Hudson)

1.4.7 Canon Laser Blood Flowmeter

To date, the Canon Laser Blood Flowmeter (CLBF) is the only retinal hemodynamic assessment device that can non-invasively measure volumetric blood flow in absolute units (μL/min)[1;77]. It is a fundus camera-based instrument that uses bidirectional laser Doppler velocimetry to measure blood flow in the retinal arterioles and venules. The system uses two lasers that permit the simultaneous quantification of vessel diameter and the velocity of erythrocytes passing through, which could not be accomplished using previous bidirectional laser Doppler velocimeters. The frequency of a 675 nm laser is shifted by moving blood cells and used to determine maximum velocity, while a 544 nm laser is used to measure the diameter of the vessel. A computer-automated tracking device is used to stabilize the lasers on the target to compensate for eye movements during data acquisition[83].

Due to variations in blood velocity observed in arterials during the cardiac cycle, a time-averaged value of v_{max} determined from the DSFS, $\overline{v_{max}}$. Since fluctuations of this nature do not occur in the venous system, $\overline{v_{max}}$ is assumed to be the same as v_{max}. The flow rate, F, is calculated from $\overline{v_{max}}$ and the cross sectional area of the vessel, s, such that

$$F = \frac{1}{2}\overline{v_{max}}s \tag{1.10}$$

The factor of 2 for the calculation of flow arises from the assumption of Poiseuille's flow. The quantity, s, is calculated from the measured diameter of the blood vessel on the assumption that the cross section is circular[28]. The CLBF has been shown to give consistent and repeatable results[89;90]. Light scatter has been

observed to affect densitometry assessment of vessel diameter, and as such, the CLBF may be of limited usefulness when used on patients with cataracts[91].

1.4.8 Scanning Laser Doppler Flowmetry

The Heidelberg Retina Flowmeter (HRF) is the only commercially available scanning laser Doppler flowmetry device. As the name implies, this device uses scanning laser technology to measure volumetric blood flow in the juxtapapillary region of the retina and the optic nerve head [92]. The optical system is confocal so it is useful for assessing planar depth[1]. The laser scans a 2560 × 2560 μm area of the retina or optic nerve head with a 785 nm laser diode. The HRF software performs a fast Fourier transform to extract the individual frequency components of the reflected light to generate a power spectrum, from which a value proportional to the total number of red blood cells times their velocity is determined. The results are displayed as perfusion maps with different where colours decode the amount of perfusion, and the parameters volume, velocity, and flow are reported in arbitrary units[83].

1.4.9 Colour Doppler Imaging

Colour Doppler imaging is another retinal hemodynamic assessment technique that uses the Doppler effect. However, while the instruments that have already been described here relate the shifted frequency of light, this technique measures the Doppler-shifted frequencies of ultrasound waves to assess the blood flow in low velocity vessels (ie. the central retinal artery and posterior ciliary artery) and high velocity vessels (ie. the ophthalmic artery), depending upon adjustable sensitivity and depth settings. A coloured representation of a B-scan ultrasound image allows visualization of blood flowing through the orbital vessels[77]. Peak systolic and end-diastolic velocities are identified and used to calculate the resistive index associated with the vascular beds perfused by the artery being measured. Colour Doppler imaging has the

advantage of being non-invasive (performed on a closed eye), and is effective in eyes with poor optical media[1]. A potential problem arises with this procedure if too much pressure is applied with the transducer, as this could cause a temporary rise in IOP which could have a confounding effect on ocular hemodynamics.

1.5 Studies in Retinal Blood Flow During Hyperoxia

It has been demonstrated in many studies that blood flow varies depending on systemic arterial oxygen tension[53;55;70;93-97;97-102]. When systemic hyperoxia is initiated by manipulating inspired gases, local increases in O_2 tension elicit the vascular reactivity response in the retinal arterioles, causing vasoconstriction to reduce blood flow in order to maintain a steady supply of O_2 to the retina[42]. The vascular reactivity limits of the retinal vasculature were investigated by maximizing systemic hyperoxia (pure O_2 breathing) in most studies[53;70;93-101], however, only a few studies demonstrated the effects of varying the pO_2 of the inhaled gas[98;100]. Several problems are inherent in these studies including the lack of standardization of hyperoxia. Without measuring arterial pO_2 or at least a surrogate indicator, it is impossible to determine whether the breathing stimulus exerted an equal vasoconstrictive influence in each subject since systemic pO_2 can vary between individuals given the same gas stimulus. In addition, these studies failed to control against changes in pCO_2[53;70;93-96;98-101]. Given the vasodilatory effect of CO_2 on the retinal vasculature, changes in pCO_2 confounded the results[66;96]. Isocapnia was maintained in only a few studies in which hyperoxia was the primary stimulus[55;97;102]. This can be achieved using a sequential re-breathing circuit in which fresh gas was enriched with CO_2 from rebreathed gas to prevent hyperoxia-induced hypocapnia[102] or by supplementing pure O_2 with CO_2[97]. In addition to better control of the stimulus, this method improved hemodynamic measurements by reducing variability in the data [102]. One study has reported a linear relationship between systemic pO_2 and retinal hemodynamics[98], however, in

studies that only compared pure O_2 versus air breathing, a curvilinear relationship could not be excluded [53;70;93-101].

There is consensus among the studies that hyperoxia produces a profound reduction in retinal blood flow[53;55;70;93-97;97-102]. The rate of blood flow during hyperoxia relative to normoxia can be assessed, however, the methods of ocular hemodynamic measurements (1.4) each have unique limitations including simplifications or assumptions of ocular blood flow characteristics, or the inability to measure blood flow in absolute units which prevent the assessment of retinal blood flow for each of the different conditions in absolute terms[1;77;103]. Each hemodynamic measuring device assesses a different part of the ocular circulation[98]. Vascular reactivity varies with regional differences within the retina[97], further complicating such comparisons. These data should therefore be interpreted with an adequate understanding of the techniques that are used and the anatomy and physiology of ocular blood flow

1.6 Summary

As the retina is the only location within the body where internal blood vessels can be viewed directly and non-invasively, it presents as a unique opportunity for the study of hemodynamics. The anatomy and physiology of ocular blood flow, with particular attention to blood flow in the retina has been reviewed here. The retina is the most metabolically active tissue in the body while also being particularly vulnerable to periods of low perfusion due to the peculiarities of its anatomy, physiology, and function. As such, proper control of blood flow to the retina to ensure adequate delivery of nutrients, removal of wastes, and oxygenation are essential to maintaining the health of the eye.

To this end, many techniques have been developed to assess *in vivo* ocular hemodynamics for clinical and experimental purposes. This is by no means an exhaustive review of the devices and techniques that have

been devised to assess ocular hemodynamics. It is, however, a sample of some of the techniques that have been used to study the blood vessels and capillary beds of the retina, the choroid, and the optic nerve head. These have been used to measure baseline hemodynamics along with various stimuli such as flickering light and inspired gases to assess the reactivity of the vessels in both health and disease. A decline in the ability of the vasculature to regulate perfusion in the face of these stimuli are part of the pathogenesis or sequelae of various eye disease such as diabetic retinopathy, age-related macular degeneration, and glaucoma. Each of the techniques provide a view of what is happening in different vascular beds, however, since blood flow is measured in arbitrary units in most cases, it is difficult to relate the findings between the various studies that have been published. Nonetheless, assessment of ocular hemodynamics in its various forms contributes to our understanding of the basic physiology of the eye and how the eye is affected by disease.

Chapter 2
Rationale for Investigating Retinal Vascular Reactivity in Isocapnic Hyperoxic Conditions

The retinal arterioles are resistance vessels that control the rate of blood flow by altering lumen diameter. A reduction in diameter will reduce blood flow, while an increase in diameter will increase blood flow. In the inner retina, diameter is modified through the influence of the myogenic response, endothelium-derived factors, local hormones, and tissue metabolites in the absence of sympathetic innervation. These mechanisms ensure a steady supply of oxygen to the retina to support its high metabolic needs. Vascular reactivity or metabolic autoregulation is the ability of a tissue to alter perfusion to match the O_2, CO_2, and nutrient needs[42] of the retina and is a quality exhibited by the major retinal arterioles.

Vasoconstriction and reduction in retinal blood flow in response to hyperoxia induced by increased inspired oxygen levels has been demonstrated in many studies[53;70;93-101]. Hyperoxia was induced by breathing 100% oxygen in these studies, without controlling for changes in CO_2 tension in the arterial blood[53;70;93-96;98-101]. Hemoglobin is nearly saturated in normoxic conditions in a healthy person, and breathing pure oxygen almost exclusively increases pO_2 in arterial blood by increasing the amount of O_2 dissolved in the plasma. Since oxyhemoglobin binds less CO_2 (Haldane effect)[104-106], what results is a reduction of pCO_2 in the arterial blood, an accumulation of CO_2 and bicarbonate in local tissue, which stimulate central chemoreceptors to cause hyperventilation[63;107;108]. Hyperventilation further exacerbates hypocapnia. The magnitude of the hypocapnic effect elicited during hyperoxic provocation varies substantially from one individual to the next. Since CO_2 causes vasodilation of responsive resistance vessels including retinal arterioles[66], a decrease in CO_2 during hyperoxic provocation would exaggerate the vasoconstrictive effect and confound the influence of hyperoxia on vascular reactivity. Co-

administration of CO_2 with hyperbaric O_2 elicits a smaller vasoconstrictive effect than pure O_2 breathing [70;96;109], demonstrating this hypocapnic effect. The compounded vasoconstrictive effect makes data from previous studies difficult to interpret, emphasizing the importance of maintaining isocapnia during hyperoxic experiments so that the effect of O_2 breathing can be isolated from CO_2 drift.

A sequential rebreathing circuit was developed to standardize O_2 provocation defined by fractional-expired O_2 (FeO_2) delivery, while also preventing the reduction of end-tidal CO_2 ($ETCO_2$). This is achieved using two gas reservoirs interconnected by a single positive end expiratory pressure (PEEP) valve, which allows for rebreathed gas from one of the reservoirs to mix with gas from the fresh gas reservoir. The flow rate of fresh gas is adjusted such that $ETCO_2$ is maintained at the subject's homeostatic level when breathing through the mask. The mixing of fresh and rebreathed gases ensures that the subject breathes enough CO_2 to prevent hypocapnia. Regulation of end-tidal concentrations of O_2 and CO_2 in this way reduced the variability of retinal hemodynamic measurements compared to other methods of gas delivery[102]. This technique is manually-operated and must be continuously monitored by the experimenter for possible $ETCO_2$ drifts, and fresh gas flow is adjusted accordingly. Normoxia and hyperoxia are stimulated using air and 100% O_2 gas, respectively, and different incremental increases of O_2 between normoxia and hyperoxia (defined in this method as 100% O_2) could not be achieved without utilizing a special gas mix.

A recently developed computer-controlled gas delivery system can compensate for some of the limitations of the manually-operated system. An almost identical sequential rebreathing circuit was used, however, the O_2 and CO_2 demand to match a user-input $PetCO_2$ and $PetO_2$ is automatically calculated by the delivery system, and is adjusted on a breath-by-breath basis to stabilize the levels of O_2 and CO_2 in the systemic circulation. Three source gases with different proportions of O_2, CO_2, and N_2 are mixed together

to achieve the user-input targets while also ensuring that a safe minimum of N_2 and O_2, or safe maximum of CO_2 are delivered to the participant. Through better control of both pO_2 and pCO_2, the computer-controlled gas sequencer permits sequential changes in $PetCO_2$ and $PetO_2$ and is thought to produce more reliable results when measuring retinal vascular reactivity. It is also capable of faster transitions between gas challenges allowing systemic blood gas to equilibrate more quickly and accurately than with the previous method.

Due to the benefits of the computer-controlled gas delivery system, it is likely to replace the manually-operated system in retinal vascular reactivity studies in our lab. However, since previous studies investigating the retinal vascular response to hyperoxia were conducted with the manually-operated system, it was important to compare the performance of both gas delivery systems in terms of retinal hemodynamic measurements. This is the rationale for the study described in Chapter 3 of this thesis. One measurable difference between the two gas delivery methods is in the delivery of O_2 during hyperoxia. The manually-operated system can achieve FeO_2 levels up to approximately 85%, a level which can vary greatly between participants as a result of differences in tidal volume. However, the computer-controlled system can only achieve approximately 70% FeO_2 while maintaining the comfort and safety of the participant but with greater consistency between participants. Retinal arteriolar diameter, blood velocity, and blood flow were each assessed to determine how the differences in oxygen delivery between the two systems were relevant in the context of the magnitude and variability of retinal vascular reactivity to an isocapnic hyperoxic provocation. In short, the aim of Chapter 3 is to compare the retinal hemodynamic measurements obtained from two different gas delivery methods to provide insight on how data from both methods should be interpreted relative to each other.

Although the maximal FeO_2 target is lower for the computer-controlled delivery system, its main advantage in hyperoxia studies is in its capability to produce a range of FeO_2 increments between 15-65%. The aim of the study described in Chapter 4 was to investigate the retinal arteriolar response to randomised incremental hyperoxic stimuli while maintaining isocapnia. Previous studies have investigated the retinal vascular reactivity to the maximum hyperoxic response that can be attained using their respective methods[18;53;55;70;93-95;97;99;101;102;110] and compared to air breathing i.e. 15% FeO_2. Alternately, they have provided normal physiological data to demonstrate the nature of the relationship between different levels of hyperoxia and retinal vascular reactivity[96;98;100], but failed to control for hyperoxia-induced hypocapnia[53;70;93;94;98;99;101], or even deliberately altered the concentration of CO_2 in the source gases[95;96;100]. Furthermore, different levels of hyperoxia were achieved by altering the pO_2 in the source gas, but this does not account for level of gas exchange. In other words, the magnitudes of FeO_2 and $ETCO_2$ were not standardized in these studies. The primary goal of the study described in Chapter 4 is to determine the relationship between incremental hyperoxia during isocapnia and vascular reactivity in the retinal arterioles using standardized FeO_2 increments. To the best of our knowledge, this has not been previously achieved.

The overall aim of this thesis is to evaluate different methods of stimulating isocapnic hyperoxia in retinal hemodynamic studies and to determine how retinal arterioles react at various levels of hyperoxia while ensuring isocapnia. Impairment of vascular reactivity is a hallmark of ocular diseases with vascular etiologies, including diabetic retinopathy, age-related macular degeneration and glaucoma. A better understanding of the experimental methods and physiological relationships behind hyperoxic provocation and the standardization of these protocols will improve the quality of the hemodynamic data and its meaningful interpretation.

Chapter 3
Comparison of Gas Delivery Systems on the Outcome of Retinal Vascular Reactivity Measurements to Isocapnic Hyperoxia

3.1 Abstract

Purpose: The aim of the study was to compare the magnitude and variability of the retinal vascular reactivity response to an isocapnic hyperoxia stimulus delivered using a manually-operated method to that of a newly developed computer-controlled gas sequencer.

Methods: The sample comprised 10 young, healthy subjects. During a single visit, subjects inhaled gases in a sequence of normoxic baseline, isocapnic hyperoxia, and normoxic recovery, using both gas delivery systems in random order. End-tidal partial pressure of carbon dioxide ($ETCO_2$) and fractional expired oxygen (FeO_2) were continuously monitored. Blood flow was derived from retinal arteriolar diameter and simultaneous blood velocity measurements of the superior temporal arteriole, acquired at 1-minute intervals during each of the phases of the gas protocol.

Results: There was no interaction effect between the phases and gas delivery methods ($p = 0.7718$), but $ETCO_2$ was significantly reduced during hyperoxia ($p = 0.0002$) for both methods. The two systems differed in terms of FeO_2 during hyperoxia, at a level of $85.27 \pm 0.29\%$ for the manual method, and $69.02 \pm 2.84\%$ for computer method ($p < 0.05$). Despite this difference in oxygen concentrations, there was no difference in the vascular reactivity response for diameter ($p = 0.7756$), velocity ($p = 0.1176$), and flow ($p = 0.1885$) for equivalent gas phases between the two gas delivery systems.

Conclusions: Inter-subject variability for virtually all retinal hemodynamic parameters was reduced using the computer-controlled method, presumably due to a higher degree of gas control. However, due to the relatively small sample size care needs to be exercised in the interpretation of this result. A similar retinal hemodynamic response to isocapnic hyperoxia was induced using the two gas delivery systems, despite different levels of maximal FeO_2.

3.2 Introduction

Metabolic autoregulation of the retinal arterioles ensures that the oxygen supply attempts to match the metabolic activity of the retina in spite of changes in the concentration of inspired gases[42]. One unique feature of the retinal vasculature is that it lacks sympathetic innervation[32], and as a result, the influence of endothelial-derived factors and local metabolites play an important role in the regulation of vasomotor response of the resistance vessels of the retina. Retinal blood flow varies directly with the arterial partial pressure of CO_2 ($PaCO_2$) and inversely with the arterial partial pressure of O_2 (PaO2). Hyperoxia induced by O_2 breathing causes vasoconstriction in the retinal arterioles, a process which is influenced by endothelin-1 (ET-1)[57;58]. Impairment of vascular reactivity of retinal blood flow in response to hyperoxia has been demonstrated in diabetic retinopathy[18;97] and glaucoma[111].

Many experiments simply induce hyperoxia through 100% O_2 breathing[53;70;93-101]. This methodology presents a number of problems. First, it erroneously assumes that 100% O_2 breathing produces the same degree of systemic hyperoxia in all participants[112], and hence, the degree of provocation of is not standardized. Fractional expired oxygen (FeO_2) should be monitored as a surrogate measure of the partial pressure of O_2 (pO_2) in the arterial blood and O_2 delivery should be adjusted accordingly to reduce variability of the O_2 across subjects within a study. Second, hyperoxia induces hypocapnia, a condition which was not considered in many studies[63;102]. Oxyhemoglobin has a lower affinity for CO_2 binding resulting in CO_2 and bicarbonate build-up that stimulates brainstem chemoreceptors to increase the respiratory rate[107;108]. Hyperventilation worsens hypocapnia, which results in vasoconstriction at a level that is greater than that caused by hyperoxia alone[63]. In this way, the effect of hyperoxia on autoregulation is confounded in many studies by a drift in systemic CO_2 levels[53;70;93-96;98-101].

A sequential rebreathing circuit can be used to manipulate inspired and expired gases, such that during inspiration, the subject inhales a mixture of fresh gas along with a small amount of gas from a rebreathed gas reservoir [102]. This system can effectively minimize CO_2 drift during hyperoxia induction with pure O_2 breathing because it is supplemented by CO_2 from the rebreathed gas reservoir, maintaining normocapnia. However, with this method, FeO_2 cannot be standardized between study participants since normoxia and hyperoxia are induced using one standard air and 100% O_2 respectively, and FeO_2 equilibrates at different levels depending on each person's gas exchange rate. Changes in FeO_2 are controlled manually between normoxia and hyperoxia. This system has been used in a number of studies that investigated retinal vascular reactivity to isocapnic hyperoxia challenge[18;55;102].

A recently developed computer-controlled gas delivery system combined the sequential rebreathing circuit with an automated system that can simultaneously standardize FeO_2 and $ETCO_2$ across subjects in a study. This is accomplished by blending 3 different source gases and breath-by-breath monitoring of exhaled gases to adjust the relative concentrations of the source gases to achieve the user-input $ETCO_2$ and FeO_2 target levels, following a programmed time sequence. It was previously found that better control of the gas parameters reduced the variability of retinal hemodynamic measurements using a manually-operated sequential rebreathing circuit[102]. The purpose of this study was to compare the magnitude and variability of retinal hemodynamic measurements between the manually-operated and computer controlled gas delivery systems.

3.3 Materials and Methods

3.3.1 Participants

Ten healthy adults (5 men, 5 women) were enrolled in the study, ranging in age from 21 to 33 years (mean age 27.1 years, SD ± 4.43). All participants had a corrected logMAR (logarithm of the minimum angle of resolution) visual acuity of 0.0 or better. Participants were excluded if they had refractive error greater than ± 6.00 DS and/or ± 2.50 DC. They were also excluded from the study if they had a history of ocular disease or disorder, including lenticular opacity which interfered with imaging measurements[91]. The participants had no history of intraocular or refractive surgery. People with a history of systemic disease including respiratory disorders, heart or cardiovascular disease, or hypercholesterolemia were also excluded. Systemic medications with known vasoactive effects were also excluded. Since caffeine has known transient systemic vasoconstrictive effects in humans, and effects on retinal hemodynamics[113], subjects were also asked to refrain from caffeine-containing food products such as coffee, tea, chocolate for 24 hours prior to their study visit. A diminished reduction of blood flow secondary to hyperoxia has been observed in the retinal circulation of smokers, a response attributed to the long-term effects of nicotine on the sympathetic and parasympathetic nervous system[114]. As such, current smokers, or those who have smoked cigarettes within six months of the study, were also excluded from participation.

3.3.2 Pre-Data Collection Screening

Prior to data collection, a screening was performed to ensure that each participant met the study criteria. A medical history was taken, with questions pertaining to the aforementioned exclusion criteria. Blood pressure and pulse measurements were taken using a digital blood pressure monitor (Omron HEM-907, Intellisense^{TM}) to exclude patients who had high blood pressure (>140/90).

Visual acuity was measured with the Early Treatment of Diabetic Retinopathy Study (ETDRS) logMAR charts[115]. Since participants in the study are expected to have good corrected visual acuity, they were asked to start at the row in which they can comfortably read all five letters, and continue to read the letters down the chart until they could not correctly identify a minimum of three letters while wearing their spectacles. The last line that the participants could read was recorded. These measurements were taken to ensure that the participants met the vision requirement so that optical defects did not interfere with CLBF imaging.

Prior to blood flow data acquisition, a drop of fluorescein was applied to the cornea to screen the cornea and tear film for abrasions or irregularities that could interfere with imaging. Study participants were also asked if they had known allergies to the ophthalmic drops used in the study. Van Herrick's angle assessment was performed to determine the risk of anterior angle closure, prior to the use of mydriatic drops. Once it was determined that mydriasis was safe (ie. cornea to chamber ratio > 1:1/2), one drop of 1% Tropicamide was applied to the randomly chosen study eye.

3.3.3 Gas Delivery Systems

3.3.3.1 General Protocol

Participants were fitted with a face mask and a gas delivery system comprising a sequential re-breathing circuit through which they breathed a controlled mixture of gases (Figure 3-1). A transparent medical film dressing (3M™ Tegaderm™, St. Paul, MN) was used to secure the mask and to create an airtight seal around the face.

Figure 3-1. Experiment Set-up.

Participant is fitted with a face mask and rebreathing circuit. To the left of the photo (behind the participant) is the computer-controlled gas delivery system with 3 tanks of compressed gases. In the background is the manually-operated system with 3 rotometers used to control the flow of gas from two compressed tanks (air and 100% O2). To the right (in front of the participant) is the CLBF used for retinal hemodynamic measurements.

Manually-operated and computer-controlled sequencer gas delivery systems were used in random order during a single study visit. In general, a sequence consisting of a normoxic baseline, hyperoxia, and normoxic recovery, whilst maintaining isocapnia throughout, was achieved using both methods. End-tidal (end of exhalation) partial pressure of oxygen ($PetO_2$) and carbon dioxide ($PetCO_2$), which is the

maximum concentration of each gas during expiration, were sampled since these parameters reflect the arterial partial pressure of oxygen (PaO_2) and carbon dioxide ($PaCO_2$).

3.3.3.2 Sequential Rebreathing for Isocapnic Hyperoxia

A sequential rebreathing circuit consisting of a fresh gas reservoir and a rebreathed gas reservoir that are interconnected by two one-way valves and a single positive end-expiratory pressure (PEEP) valve between them (Hi-Ox80, Viasys Healthcare, Yorba Linda, CA) can be used to maintain a constant level of $ETCO_2$. The participant inhales gas from both the fresh gas and re-breathed gas reservoirs with each inhalation, and the CO_2 in the re-breathed gas essentially maintains isocapnia.

As fresh gas flows from the gas tank, it enters the fresh gas reservoir. Negative pressure from the mask produced by inhalation opens the one-way valve connected to the fresh gas reservoir, thus allowing fresh gas to enter the mask. Positive pressure from the mask produced by exhalation opens the one-way valve connected to the rebreathed gas reservoir, allowing gas to enter that chamber.

Rebreathing occurs when the participant's ventilation rate exceeds the rate of gas flow from the inspiratory limb of the system. In this situation, negative pressure from the mask opens the PEEP valve that connects the inspiratory limb with the expiratory limb. This unidirectional valve allows re-breathed gas to enter the inspiratory limb, increasing pCO_2 of the inspired gas.

The process described here is relevant to both the manually-operated and computer-controlled gas regulation systems. There are, however, several distinctions between the two systems in regulation of the gas parameters that will be described in the following sections

3.3.3.3 Manually-Operated Gas Delivery System

This system has been previously described[102], but due to the relevance of its design in this study, the details will be outlined here. The sequential rebreathing circuit for the manually-operated gas delivery system consisted of a fresh gas reservoir (750 mL) and re-breathed gas reservoir (2000 mL) as described in the previous section. Standard rotometers acted as flowmeters, to regulate the delivery of gas from two gas tanks. One tank contained 100% oxygen and the other contained air. Air was delivered to the patient during normoxic phases, ie. baseline and recovery, while oxygen was delivered to induce hyperoxia. The flow from each of the gas tanks were manually adjusted at the start of each phase until end-tidal carbon dioxide ($ETCO_2$) and fractional expired oxygen (FeO_2) levels were stabilized. Gas parameters were monitored using the Datex Ohmeda Cardiocap^{TM}/5, a rapid-response critical care monitor.

The desired flow rate of fresh gas was achieved when partial rebreathing was occurring. This was evidenced by the partial collapse of the rebreathed gas reservoir at each breath and verified by the respiratory waveform on the critical care monitor. 5% $ETCO_2$ was the target at all phases, while FeO_2 varied from 15% during normoxia to approximately 85-90% during hyperoxia (Figure 3-2). However, since the method depends upon minute ventilation, $ETCO_2$ and FeO_2 stabilized at individual homeostatic values rather than absolute targets.

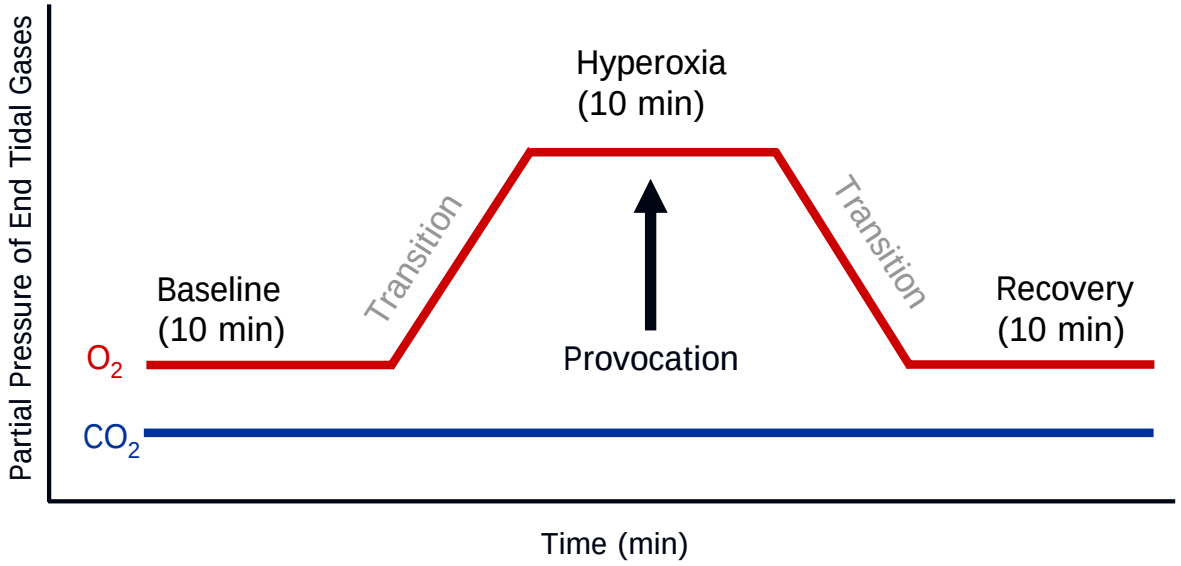

Figure 3-2. Gas Sequence for Manually-Operated Gas Delivery System.

The gradual transition in FeO_2 between phases is a feature of this method of gas delivery, as indicated by the red line (O_2). Isocapnia is maintained throughout the protocol, as indicated by the flat blue line (CO_2). Air was used during Baseline and Recovery phases while Hyperoxia was induced by administering 100% O_2.

3.3.3.4 Computer-Controlled Gas Delivery System

A similar rebreathing circuit was used for the computer-controlled gas delivery system. The same mask (Hi-Ox80, ViasysHealthcare, Yorba Linda, CA) featuring two gas reservoirs interconnected by a single PEEP valve was used. The main difference in the sequential rebreathing circuit was the expansion of gas reservoirs. The inspiratory limb consisted of two continuous fresh gas reservoirs (1500 mL combined volume) and expiratory limb consisted of two continuous re-breathed gas reservoirs (4000 mL). The

potential volume of the fresh gas reservoir was greater than the actual volume of gas it contained, given the variable flow rate of gases between participants to achieve end-tidal gas parameters.

The computer-controlled method of regulating end-tidal carbon dioxide and oxygen levels was unique from the manually-operated method. Metabolic parameters, consisting of oxygen uptake rate (VO_2) and carbon dioxide elimination rate (VCO_2), were sampled through the built-in gas analyzer prior to the start of the experiment. These measurements are related to individual metabolic rate and physiological deadspace, the component of ventilation that does not participate in gas exchange. The algorithm controlling gas delivery accounts for these parameters when calculating the amount and mix of gas required by the individual.

Unlike the manually-operated apparatus, it induces a target $PetO_2$ and $PetCO_2$ of the subject independent of each other and independent of minute ventilation. Sequential changes to different target $PetO_2$ and $PetCO_2$ are controlled by the Up-Down Program, a software package designed to analyze breath-by-breath changes in $PetO_2$ and $PetCO_2$ and vary the delivery of gas through the apparatus in order to stabilize both parameters during each of the phases. The sequence of normoxia, hyperoxia, and normoxic recovery at isocapnia were pre-programmed using the Up-Down Program. The targeted $PetCO_2$ during all phases was 38 mmHg, which corresponds to approximately 5% $ETCO_2$, ie. baseline $PetCO_2$ was normalized across individuals. The targeted FeO_2 level was approximately 14% (100 mmHg $PetO_2$) for both baseline and recovery phases, and 70% (500 mmHg $PetO_2$) during hyperoxia (Figure 3-3). Sequential changes to target $PetO_2$ and $PetCO_2$ occur with shorter transition times using this method, without the need to change minute ventilation on the part of the subject. However, when changes in minute ventilation occurred, the delivery of fresh gas was automatically altered to maintain $PetO_2$ and $PetCO_2$ at target levels. This occurred because of three special features of the computer-controlled gas

sequencer:

1) It calculates, for a given total flow, fractional concentrations of O_2 and CO_2 entering the sequential gas delivery circuit required to attain a target $PetO_2$ and $PetCO_2$.
2) It identifies and provides the total flow by mixing component flows of source gases. The source gases contain a safe minimum concentration of O_2, and/or N_2, and/or maximum of CO_2. Specifically, the source gases were 100% oxygen, air, Gas A (10% O_2, 90% N_2), and Gas B (40% CO_2, 10% O_2, 50% N_2).
3) If changes in target $PetO_2$ and $PetCO_2$ are required, it identifies and applies transient changes in the partial pressure of O_2 (PO_2) and the partial pressure CO_2 (PCO_2) in the total flow that would accelerate the change in the patient's blood gases towards the new target levels.

In this way, the computer-controlled gas sequencer apparatus allowed for full automation. However, if necessary, the operator could make adjustments throughout the protocol to override the original program[116].

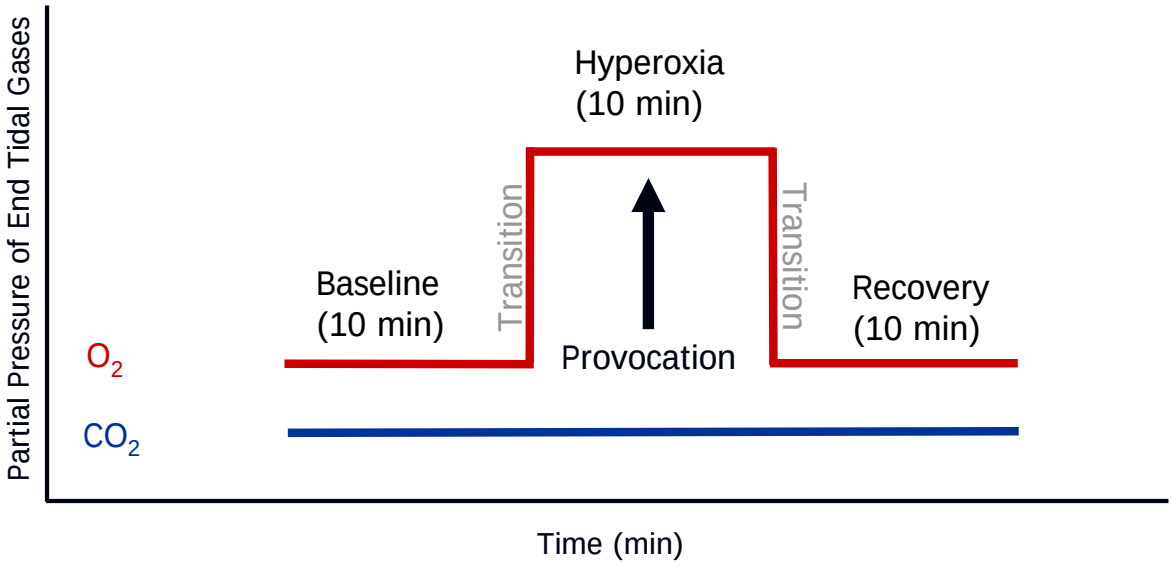

Figure 3-3. Gas Sequence for Computer-Controlled Gas Delivery System.
Square-wave transitions between phases is possible when this system is used. Isocapnia is maintained throughout the protocol, as indicated by the flat blue line (CO_2). The red line (O_2) reflects changes in FeO_2 which was targeted at 70% for the Hyperoxia phase and 14% for Baseline and Recovery phases.

3.3.4 Canon Laser Blood Flowmeter (CLBF)

The CLBF non-invasively measures volumetric retinal blood flow using bidirectional laser-Doppler flowmetry [87]. This fundus camera-based instrument provides an image of the retina which allows the operator to target a specific sampling site on an arteriole or venule. After the pupil is dilated, the participant is asked to follow the movement of the fixation target until it is in the correct position for the laser. The head of the CLBF is positioned by the operator such that two flashing yellow triangles, the corneal reflections, are in focus and aligned with the horizontal meridian of the image[117].

Two lasers are activated and measurements are made within a user-specified, 2-second time frame. The green rectangular He-Ne laser (543nm, 4-6 μW), oriented perpendicularly to the vessel axis, tracks the vessel and measures the vessel diameter. Tracking stabilizes the measurement site during small eye movements. Retinal vessel diameter is determined by computer analysis of densitometry vessel profiles taken by a linear imaging sensor every 4 milliseconds just before and after each velocity measurement, for a total of 15 vessel profiles for each 2-second sampling period.

The red oval laser diode (675 nm, 200-300 μW) light is emitted to measure the centerline velocity (mm/s) of erythrocytes. Two photomultiplier tubes separated at a fixed angle simultaneously detect Doppler-shifted light scattered by moving erythrocytes[87]. The use of bidirectional photodetectors permits the quantification of blood velocity, irrespective of the angle between the moving blood cells and reflected light. Computer analysis of the signals from the detectors determines the centerline blood velocity.

A single measurement site was chosen approximately one disc diameter from the optic nerve head in the superior retinal arteriole. The CLBF software records the exact location of the measurement site so that it is consistent for each participant within and between experiments, allowing for reliable comparisons. Measurement sites were located in a relatively straight segment of the vessel that was free from bifurcations, since Poiseuille's (non-turbulent) flow is assumed. During each of the gas phases, 6 CLBF measurements were taken after the end-tidal gases stabilized. A period of at least 10 minutes after cessation of the hyperoxic stimulus was allowed before CLBF measurements were taken since a recent study in our lab found that vasoconstriction can persist for approximately up to that length of time after hyperoxia. This ensured that no residual vasoconstriction due to hyperoxia would influence the CLBF measurements taken during the recovery phase.

3.3.5 Data Analysis

3.3.5.1 Gas Data

End-tidal gas parameters were recorded directly by either a critical care gas monitor for the manually operated system or by an in inherent feature of the computer-controlled gas delivery system, on a breath-by-breath basis. $PetO_2$ and $PetCO_2$ were reported in mmHg, and were converted to FeO_2 and $ETCO_2$, which are reported as a percentage of the atmospheric pressure. Upon plotting FeO_2 and $ETCO_2$ against time (in minutes), values derived during the transition between normoxic and hyperoxic phases were excluded. The transition phases were defined as the time interval between the initiation of a new phase by varying the concentration of the delivered gas and the time at which both FeO_2 and $ETCO_2$ were stabilized. The transition was easily identified by the shape of the waveform when the end-tidal gasses were plotted against time in a graph, and because the initiation of the stimulus between phases was carefully noted during data collection. Data points lying outside the 10^{th} and 90^{th} percentiles (ie. 3 SDs from the mean) of each phase were excluded as outliers, since they were likely the result of misinterpretation of the tidal waveforms by the gas monitor.

3.3.5.2 CLBF Data

A post-acquisition analysis of the velocity waveforms were performed using a standardized protocol to remove aberrant waveforms affected by eye movements, tear film breakup, or improper tracking of the measurement laser. Velocity waveforms were accepted if there was a minimum of one complete cardiac cycle which was not adversely affected by major eye movements, ie. more than 50 μm in each direction.

3.3.5.3 Statistical Analysis

Differences in end-tidal gas parameters ($ETCO_2$ and FeO_2) for each phase (baseline, hyperoxia, and recovery) was analyzed using repeated measures ANOVA (reANOVA). Similarly differences in retinal hemodynamic parameters (blood vessel diameter, blood velocity, and blood flow) were analyzed using reANOVA for each phase in the gas sequence. Fishers's Least Significant Difference (LSD) tests ($\alpha = 0.05$) were performed where gas phases were found to have a significant effect on either end-tidal gas or retinal hemodynamic parameters. The coefficients of variation (COV), defined as SD divided by the mean, were calculated for the stimulus variables (FeO_2, $ETCO_2$) and the response variables (arteriolar diametery, blood velocity, and blood flow) during each treatment (gas delivery method by phase) to compare the variability between each gas delivery method.

3.3.6 Results

3.3.6.1 End-Tidal Gas Parameters

Table 3-1 summarizes the means and SDs of the $ETCO_2$ and FeO_2 during each phase of the gas protocols for each gas delivery method. The manually-controlled and computer-controlled gas delivery systems were significantly different for both $ETCO_2$ ($p < 0.0001$) and FeO_2 ($p < 0.0001$).

There was no interaction effect between the phases and gas delivery methods ($p = 0.7718$), but the effect of phase was found to be significant ($p = 0.0002$). *Post hoc* t-tests (LSD) showed that $ETCO_2$ was significantly reduced during hyperoxia ($p < 0.05$) using both gas delivery systems. However, the change in $ETCO_2$ was less than 1%. The interaction effect between the phases and gas delivery method was significant for FeO_2 ($p < 0.0001$). During normoxia (i.e. baseline and recovery phases), FeO_2 values were comparable for both gas delivery methods. The interaction effect can be attributed to the hyperoxia phases

($p < 0.001$) in which 85.27 ± 0.29% FeO_2 was achieved using the manually-controlled method, while only 69.02 ± 2.84% FeO_2 was achieved using the computer-controlled method. All other comparisons of baseline and recovery FeO_2 values between gas delivery methods were not significantly different.

The variability of each gas delivery method, ie. the ability of each method to produce reliable end-tidal gas targets between individuals, was evaluated using coefficients of variation (COV), summarized in Table 3-2. Generally, the variability of end-tidal gas parameters was similar between the two methods. However, since $ETCO_2$ levels could not be normalized using the manually-controlled method, the outliers represent individuals who have higher or lower homeostatic $ETCO_2$ levels (Figure 3-4). In contrast, the absence of outliers for the $ETCO_2$ using the computer-controlled method demonstrates that this method was able to achieve a similar target level for all participants. The coefficients of variation were also similar for both methods for FeO_2, as shown in Table 3-2. The presence of extreme outliers accompanying a smaller range for the computer-controlled method suggests that it is also more capable of regulating FeO_2, but that approximately 70% FeO_2 represents the upper hyperoxic limit using this technique (Figure 3-5).

Table 3-1. Summary of End-Tidal Gas Parameters

	Manually-Operated			***Computer-Controlled***		
	Baseline	***Hyperoxia***	***Recovery***	***Baseline***	***Hyperoxia***	***Recovery***
$ETCO_2$	5.02 ± 0.23	4.95 ± 0.21	5.01 ± 0.22	5.55 ± 0.33	5.49 ± 0.29	5.52 ± 0.33
FeO_2	15.05 ± 0.29	85.27 ± 5.61	15.17 ± 0.21	14.61 ± 1.23	69.02 ± 2.84	14.22 ± 0.21

Values are expressed as mean % ± SD (n =10).

Table 3-2. Coefficients of Variation for End-Tidal Gas Parameters

	Manually-Operated			*Computer-Controlled*		
	Baseline	***Hyperoxia***	***Recovery***	***Baseline***	***Hyperoxia***	***Recovery***
$ETCO_2$	4.7	4.2	4.3	6.0	6.4	6.1
FeO_2	1.9	6.6	1.4	1.7	4.1	1.4

Values are expressed as %.

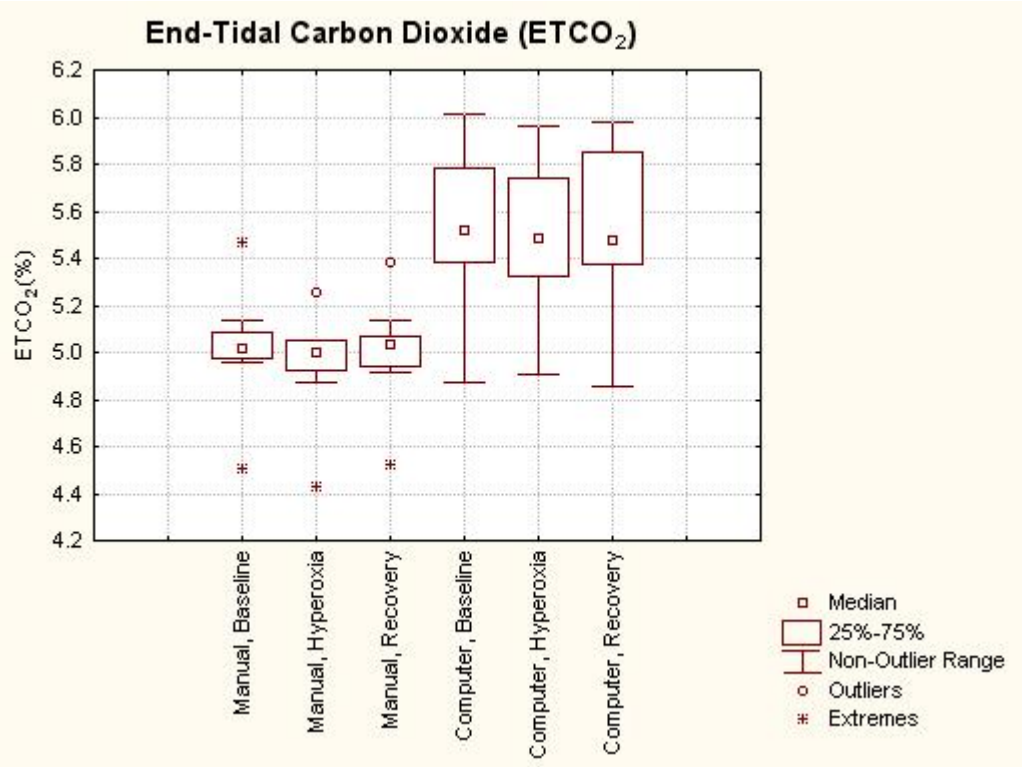

Figure 3-4. Boxplots of $ETCO_2$ at Each Phase for Both Gas Delivery Systems.

The non-outlier range (whiskers) is defined as 1.5H below the 25th percentile or above the 75th percentile, where H is the height of the box or the interquartile range. Outliers are denoted by open circles (○). Extreme outliers are denoted by asterisks (*), indicating that the values fall 3H below the 25th percentile or above the 75th percentile.

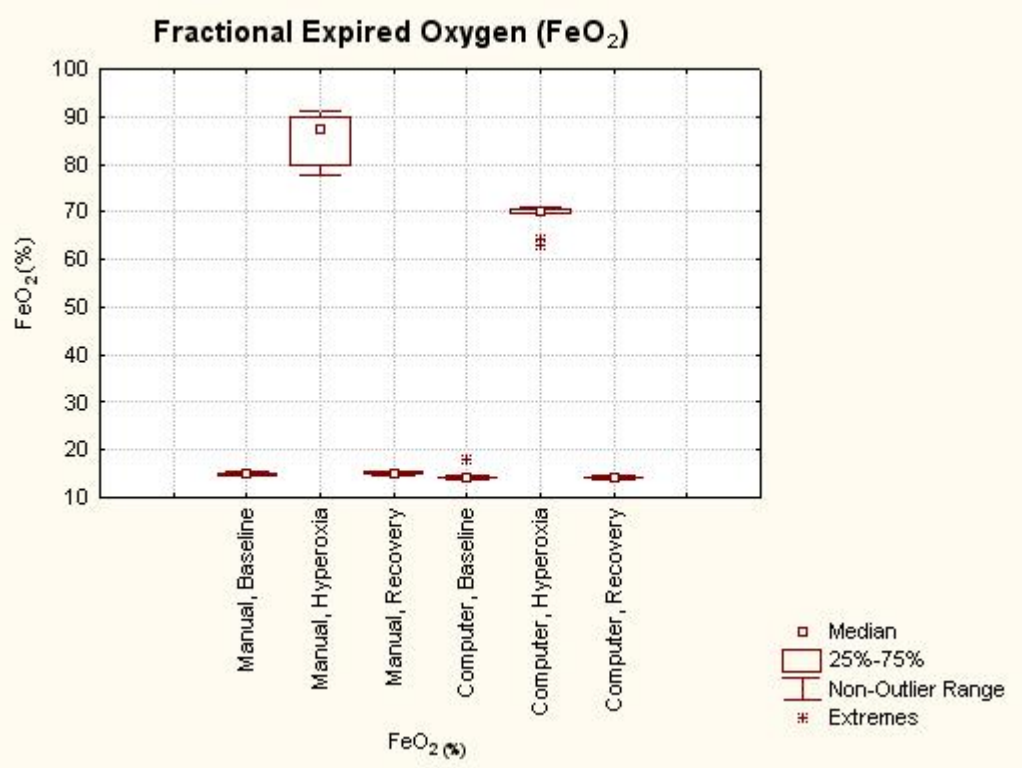

Figure 3-5. Boxplots of FeO_2 at Each Phase for Both Gas Delivery Systems.

The non-outlier range (whiskers) is defined as 1.5H below the 25th percentile or above the 75th percentile, where H is the height of the box or the interquartile range. Extreme outliers are denoted by asterisks (*), indicating that the values fall 3H below the 25th percentile or above the 75th percentile.

3.3.6.2 Retinal Hemodynamics

A reduction in arteriolar diameter, blood velocity, and blood flow was observed in the hyperoxia phase for both gas delivery methods. The difference between the two gas delivery methods were not statistically significant in terms of the response for diameter ($p = 0.9741$), velocity ($p = 0.1484$), or flow ($p = 0.1176$). Additionally, there was no interaction effect between gas delivery method and phase for diameter ($p = 0.7756$), velocity ($p = 0.1176$), or flow ($p = 0.1885$). In other words, retinal hemodynamics responded similarly during corresponding phases between the two gas delivery methods. However, the effect of phase was significant ($p < 0.0001$). *Post hoc* Fisher's LSD identified significant reductions in diameter ($p < 0.05$), velocity ($p < 0.05$), and flow ($p < 0.05$) during hyperoxic provocation, when compared to baseline and recovery values using both methods. The mean effect during baseline and recovery for diameter ($p > 0.05$), velocity ($p > 0.05$), and flow ($p > 0.05$) were not significantly different for both gas delivery phases.

The means and SDs of retinal hemodynamic parameters are reported in Table 3-1. Although the gas delivery methods did not produce significantly different retinal hemodynamic results, there was a trend toward a greater reduction in arteriolar diameter, blood velocity, and blood flow using the manually-controlled system. Between baseline and hyperoxia, mean arteriolar diameter decreased by 7.8% for the manually-controlled system, and by 7.2% for the computer-controlled system. Mean blood velocity decreased by 39.6% and 28.5% for manually-controlled and computer-controlled gas systems, respectively. Similarly, mean blood flow decreased by 48.4% and 38.0%, respectively.

Table 3-3. Summary of Retinal Hemodynamic Parameters

	Manually-Operated			*Computer-Controlled*		
	Baseline	***Hyperoxia***	***Recovery***	***Baseline***	***Hyperoxia***	***Recovery***
Arteriolar Diameter (µm)	110.1 ± 9.7	101.5 ± 12.9	109.1 ± 11.1	110.0 ± 9.2	102.1 ± 10.5	108.7 ± 9.4
Blood Velocity (mm/s)	32.3 ± 8.4	19.5 ± 6.0	30.6 ± 6.2	31.2 ± 5.9	22.3 ± 4.9	33.6 ± 7.8
Blood Flow (µL/min)	9.5 ± 3.4	4.9 ± 2.0	8.9 ± 3.1	9.2 ± 2.9	5.7 ± 1.9	9.5 ± 3.0

Values expressed as mean ± SD (n = 10)

The coefficients of variation for hemodynamic measurements, summarized in Table 3-4, were similar between the two gas delivery methods but were consistently lower in all cases for the computer-controlled method, with blood velocity during recovery being the only exception. Lower variability of hemodynamic measurements produced using the computer-controlled method is especially apparent during hyperoxia, where smaller changes from baseline occurred. In that particular situation, mean effect values were greater and standard deviations were smaller compared to the values produced using the manually-controlled method, resulting in smaller coefficients of variation. Boxplots of retinal hemodynamic parameters (Figure 3-6, Figure 3-7, Figure 3-8) show the presence of outliers when gas was delivered using the manually-controlled gas delivery system, further demonstrating higher variability of measurements using this method.

Table 3-4. Coefficients of Variation for Retinal Hemodynamics

	Manually-Operated			*Computer-Controlled*		
	Baseline	***Hyperoxia***	***Recovery***	***Baseline***	***Hyperoxia***	***Recovery***
Arteriolar Diameter (μm)	8.8	12.6	10.2	8.4	10.3	8.6
Blood Velocity (mm/s)	25.9	30.9	20.4	19.0	21.7	23.1
Blood Flow (μL/min)	36.1	41.5	35.3	31.5	32.8	31.5

Values expressed as %.

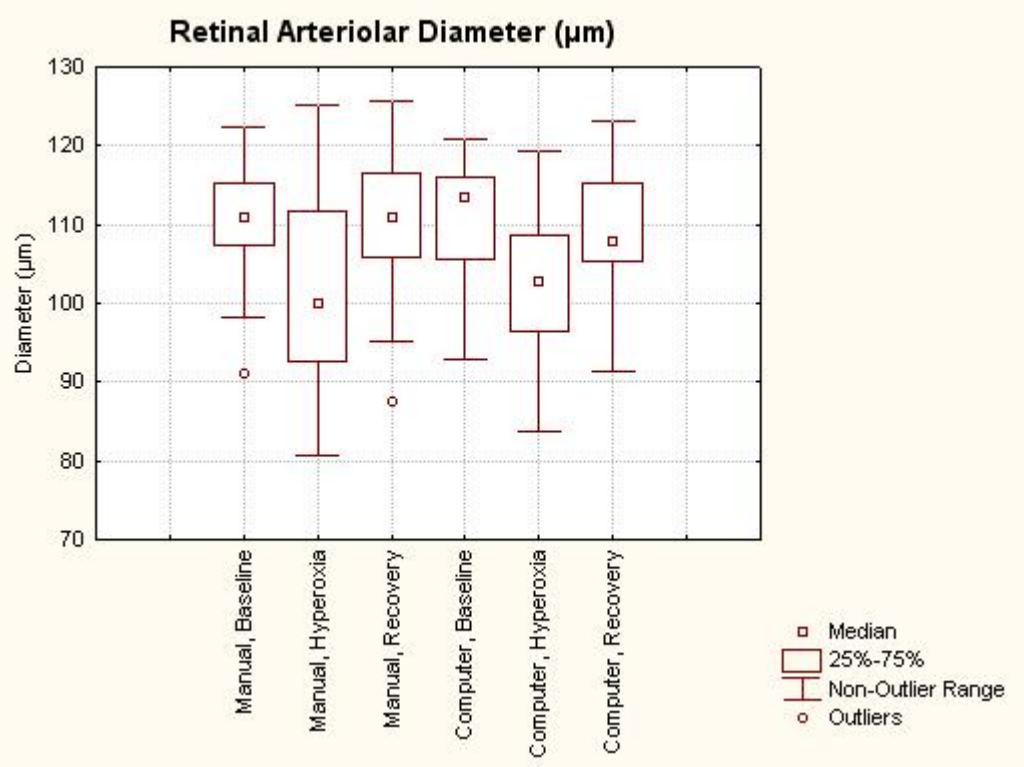

Figure 3-6. Boxplot of Retinal Arteriolar Diameter at Each Phase for Both Gas Delivery Systems. The non-outlier range (whiskers) is defined as 1.5H below the 25th percentile or above the 75th percentile, where H is the height of the box or the interquartile range. Outliers are values that lie beyond the non-outlier range and are denoted by open circles (○).

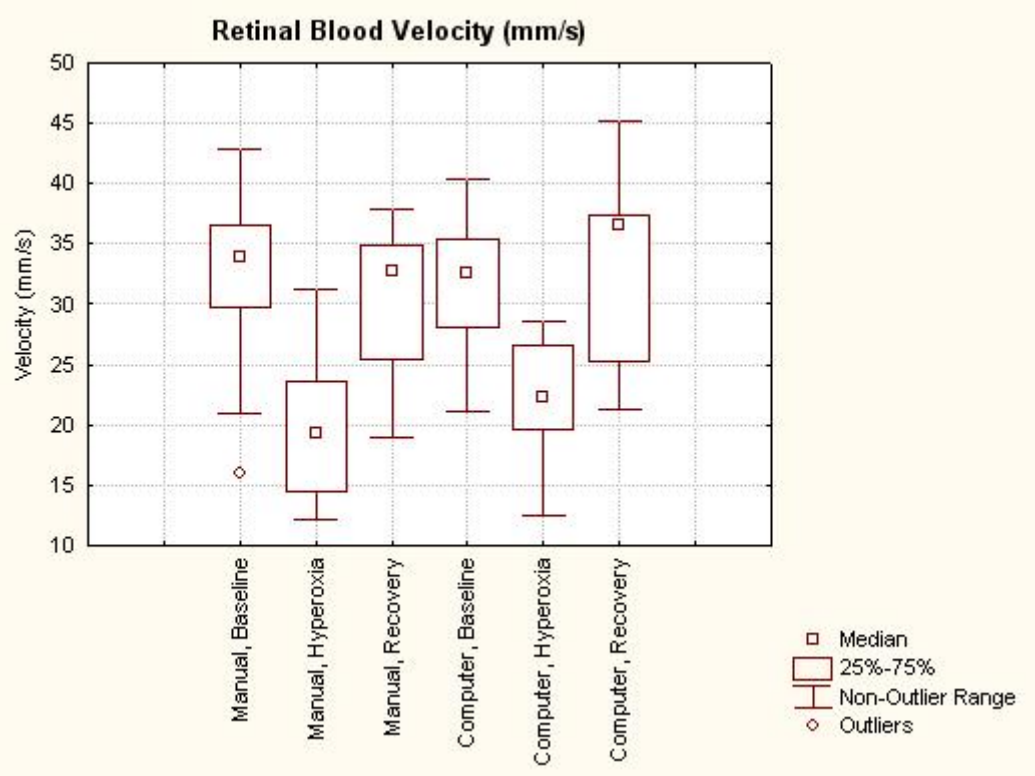

Figure 3-7. Boxplot of Blood Velocity at Each Phase for Both Gas Delivery Systems.

The non-outlier range (whiskers) is defined as 1.5H below the 25th percentile or above the 75th percentile, where H is the height of the box or the interquartile range. Outliers are values that lie beyond the non-outlier range and are denoted by open circles (○).

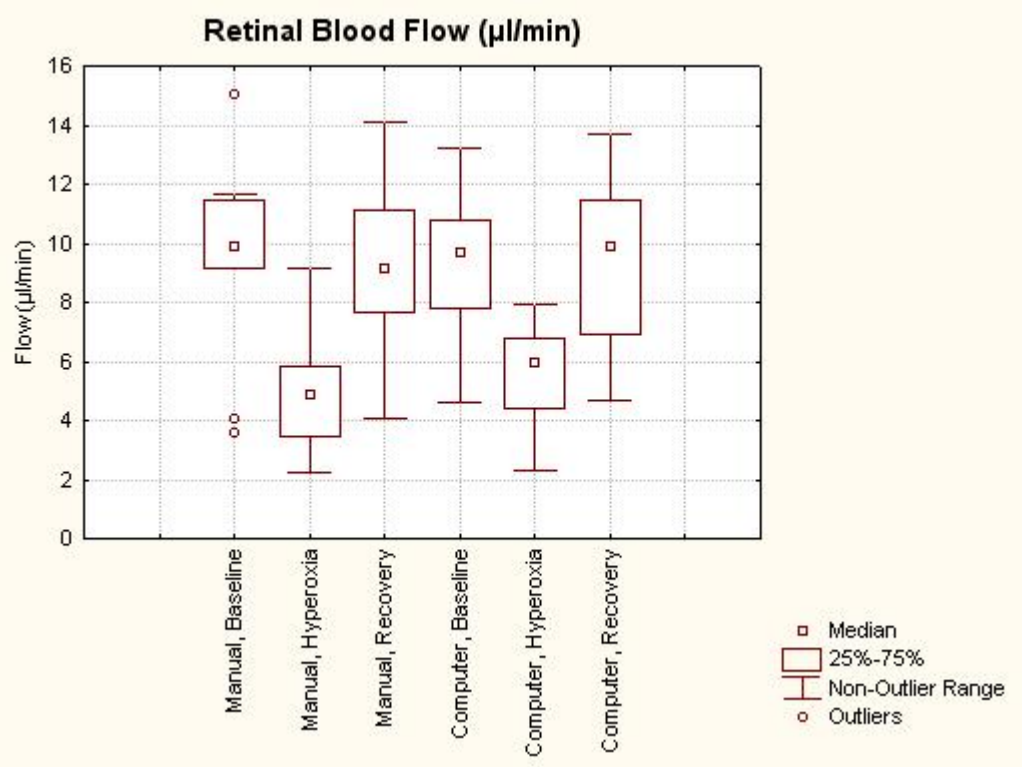

Figure 3-8. Boxplot of Blood Flow at Each Phase for Both Gas Delivery Systems.

The non-outlier range (whiskers) is defined as 1.5H below the 25th percentile or above the 75th percentile, where H is the height of the box or the interquartile range. Outliers are values that lie beyond the non-outlier range and are denoted by open circles (○).

3.4 Discussion

This study compared retinal vascular reactivity during an isocapnic hyperoxic provocation administered using a manually-controlled gas delivery system to that of a newly-developed computer-controlled method. The purpose of this investigation was to determine the impact of the new innovations including independent control of end-tidal carbon dioxide and oxygen targets and automatic breath-by-breath gas adjustments on retinal hemodynamic parameters measured using the CLBF.

It is acknowledged that the FeO_2 levels that could be achieved using the two gas delivery systems would differ simply due to methodology. The manually-controlled method achieved the maximal stable FeO_2 when 100% oxygen was delivered using a sequential rebreathing circuit (~85% FeO_2), compared to the computer-controlled method, in which a 70% FeO_2 (500 mmHg $PetO_2$) target was maintained. Rather than attempting to match the targets between methods, as it would be difficult to manipulate FeO_2 manually to reliably maintain 70% FeO_2 during hyperoxia, the maximum attainable FeO_2 for both methods was compared in this study. The latter comparison is meaningful since the motivation for this study was to examine the relationship between past studies in our laboratory [18;110]. These studies used an isocapnic hyperoxic provocation induced using the manually-controlled gas delivery system while our current studies employ the computer-controlled method. Statistical analysis confirmed that FeO_2 levels differed between the two methods during the hyperoxic provocation.

The target for the computer-controlled method is the maximal end-tidal oxygen level that can be achieved using this technique. We are confident that this is the case given the distribution of the FeO_2 data around the median during the hyperoxia phase, shown in Figure 3-5. Extremely tight regulation of FeO_2 during hyperoxia was evidenced by the small range (< 1%) between the 25^{th} and 75^{th} percentiles, and the presence of extreme outliers only below the median. In these cases, participants were unable to achieve

the 70% FeO_2 target with the computer-controlled method, or experienced slight discomfort, and the target had to be adjusted accordingly. This upper limit is imposed by the fact that a gas mix consisting of safe minimum levels of O_2 and N_2, and safe maximum levels of CO_2 for respiration are administered at all times. Multiple breaths are required to exchange most of the alveolar air since the volume of alveolar air that is replaced by atmospheric air (administered gas in this case) with each breath is only one seventh of the total alveolar volume [118]. On this principle, it would be impossible to attain square-wave transitions between phases while avoiding $ETCO_2$ drift, which is one of the characteristic goals of the computer-controlled method, especially given the magnitude of change in FeO_2 required in the transition between the baseline and hyperoxic levels defined in this study. Even if higher FeO_2 levels were targeted at the expense of the square-wave transitions, the present data suggests that it would be unattainable using the first generation of the computer-controlled gas delivery instrument. Furthermore, sustained exposure to high concentrations of oxygen elicits hyperventilation [106]. To achieve FeO_2 targets as high as the levels produced by the manually-operated method using the computer-controlled method, the increased effort due to hyperventilation would make it intolerable for participants.

Participants did not report any discomfort using the manually-controlled method of gas delivery, despite higher FeO_2. Both systems were free-breathing rather than forced ventilation; however, the differences in the participant experience could perhaps be attributed to a higher standardized gas flow rate in the computer-controlled system, whereas with the manually-controlled system, the flow rate was driven by minute ventilation which is variable between individuals.

Similarly, differences between the two gas delivery systems were also identified for $ETCO_2$ levels, mainly due to methodology. Each participant's normal $ETCO_2$ was maintained only through sequential rebreathing using the manually-controlled system. In contrast, $ETCO_2$ levels can be specifically targeted

and regulated on a breath-by-breath basis by combining the sequential rebreathing circuit with the computer-controlled method. While both gas delivery methods include a fresh gas and a rebreathed gas component, and the flow rate of each gas can be adjusted within phases, it is only with the computer-controlled method that the gas mix can be reliably varied within a phase. As a result of this innovation, fewer adjustments have to be made by the user, i.e. to adjust the flow rate in the manually-controlled method or user-entered target overrides for the computer-controlled method, to maintain stable levels using the computer-controlled method.

Although $ETCO_2$ was significantly lower during the hyperoxic phase using both methods, the magnitude of change is physiologically negligible. A reduction of less than 1% $ETCO_2$ during hyperoxia, as observed here, is in agreement with other studies involving an isocapnic hyperoxic provocation [18;55;102]. Minor drifts in $ETCO_2$ are virtually unavoidable when inspired oxygen is increased, particularly at maximal levels. Exposure to higher levels of oxygen during hyperoxia induces an increase in ventilation, increasing the rate of carbon dioxide elimination[105;106], especially if isocapnia is maintained[106]. The paradoxic rise in ventilation rate can be partly explained by the Haldane effect, whereby increased oxygen tension reduces carbon dioxide-hemoglobin binding[104-106]. Furthermore, the constrictor effect of high oxygen tension slows the circulation through the cells of the respiratory centre, leading to the accumulation of the acid products of metabolism and oxygen free radicals that stimulate brainstem CO_2/H^+ chemoreceptors due to the accumulation of the acid products of cell metabolism, thus affecting central nervous control of respiration [107;108]. However, sequential rebreathing, which passively matches the increases in minute ventilation with inhaled carbon dioxide prevents a more pronounced $ETCO_2$ reduction that would be observed with non-rebreathing techniques of gas delivery[102;119]. Sequential rebreathing is incorporated into both of the gas delivery systems studied here, although the computer-controlled method incorporates delivery of a specific fresh gas mix to further compensate for $ETCO_2$ drift. As such, fluctuations in

$ETCO_2$ were minimized to physiologically insignificant levels in this study. Furthermore, previous studies on the effect of hypercapnia on retinal hemodynamics have induced a change of approximately 15% $ETCO_2$ [68;95;120]. As such, isocapnia was essentially maintained and any changes in vessel diameter, blood velocity, and blood flow can reliably be attributed to variations in inspired oxygen levels.

Retinal vascular reactivity measurements in response to isocapnic hyperoxia induced by the manually-controlled gas delivery system were in agreement with a previous study on healthy participants using the CLBF [55]. The $ETCO_2$ and FeO_2 levels attained during normoxic (baseline and recovery) and hyperoxic phases were comparable to those achieved in that previous study which used the manually-controlled gas delivery system [55], validating the data acquired in this study. We found that there was essentially no difference in the mean effect of end-tidal gas concentrations achieved using both gas delivery methods, with the exception of FeO_2 during hyperoxia. As such, it was not surprising that there was no significant difference in retinal hemodynamic parameters when comparing baseline and recovery measurements for both systems.

Interestingly, despite a significant interaction effect between gas delivery systems and gas phase during hyperoxia (ie. FeO_2 was significantly different between the two gas delivery systems during that phase), it did not produce statistically different effects on retinal hemodynamics between the systems during hyperoxia. However, compared to baseline values, there was a trend toward higher arteriolar diameter, blood velocity, and blood flow when comparing means and SDs for the computer-controlled than the manually-controlled gas delivery system during hyperoxia (Table 3-3). These differences are subtle, as it is evident in the boxplots Figure 3-6, Figure 3-7, and Figure 3-6. When comparing the two gas delivery systems that the interquartile ranges of the hemodynamic parameters overlapped during hyperoxia.

An important finding from this study was the reduced variability in hemodynamic parameters produced during each phase using a gas stimulus administered by the computer-controlled gas delivery system. This finding has an important implication in terms of experimental design. With reduced variability, there is greater sensitivity to detecting differences between and changes between groups. It is expected, then, that a smaller sample size would be required to achieve adequate power for detecting a statistiscal difference.

A comparison between the two gas delivery systems has not been previously attempted, and as such, this was conducted as a pilot study to determine the amount of variation that can be expected with the mean effect sizes. It cannot be dismissed that a larger sample size might reveal significant differences in hemodynamic parameters during hyperoxia. With the current sample size of 10, post-hoc estimation of the statistical power of the test to reveal a difference in retinal blood flow between the two methods during hyperoxia is 51.5%. Based on the data from this study, it was determined that a sample size of 18 would have adequate power (80.7%) to show a difference, assuming that a true difference does exist. However, since this is the first study to compare the two gas delivery systems, there was no existing data suggesting an adequate sample size. Hence, no further participants were recruited into the study to increase the sample size as a result of this analysis.

Oxygen is not exclusively delivered through the retinal vasculature as it has been shown that hyperoxic ventilation can partly overcome intraretinal anoxia during retinal artery occlusion[121]. Microelectrode studies have characterized oxygen distribution through the retina during systemic hyperoxia in several animal models including rat[122], mouse[123], rabbit[124], cat[125]. Studies of this nature have been limited to species with avascular retinas, or the occlusion of the retinal artery in species with vascular retinas. A multi-layer model of oxygen distribution and consumption in the retina has demonstrated an oxygen gradient in which choroidal oxygen tension is approximately double that of pre-retina [123]. The inner

segments of photoreceptors, outer plexiform layer, and inner plexiform layer are the dominant oxygen consumers in the retina due to the high oxygen and energy requirements of synaptic activity and restoring ionic gradients [121]. The stability of oxygen consumption during systemic hyperoxia, despite a four-fold increase in choroidal oxygen delivery, suggests that inner retinal oxygen consumption dramatically increases under such conditions in the intact retina (ie. free from retinal arterial occlusion) [126]. Furthermore, while carbon dioxide seems to modulate choroidal blood flow, oxygen tension does not have an effect[109;127;128]. Interestingly, since periarteriolar oxygen tension in the retina has been found to always be greater than in the choroid, hyperoxia-induced vasoconstriction is still largely mediated by local oxygen tension rather than oxygen diffusing from the choroid[129]. The contribution of choroidal oxygen to retinal arteriolar vasoconstriction cannot be resolved using the current study's methods. However, perhaps the degree of oxygen uptake and diffusion to the inner retina from the choroid in response to different levels of systemic hyperoxia may partially account for the similar retinal blood flow response to different levels of inspired oxygen.

It is also possible that increased oxygen delivery, beyond a certain threshold level, has no additional vasoactive effect on retinal circulation. The choroid can adequately supply the inner retina with oxygen independently of the retinal circulation during hyperbaric oxygen breathing [59;130]. Dollery et. al. [59] explains that once the arterial oxygen tension exceeds 270 mmHg, the capacity for hemoglobin to buffer against changes in oxygen pressure is lost, further reducing the low arteriovenous difference in the choroid. In spite of this, complete closure on exposure to oxygen seems to be confined to immature vessels [131]. Although many studies have investigated the effects of hyperoxia on retinal hemodynamics, hyperoxia was induced by breathing 100% oxygen, few studies have shown the effects of smaller increases in inspired oxygen on retinal blood flow. Given the capability of the computer-controlled gas

delivery system used in this study to specifically target various concentrations of inspired gas, it is ideal to provide data on the degree of retinal vascular reactivity at various levels of isocapnic hyperoxia.

Chapter 4
Retinal Hemodynamic Response to Incremental Changes in Hyperoxic Stimuli During Isocapnia

4.1 Abstract

Purpose: The high metabolic needs of the retina necessitate an efficient and precisely regulated mechanism in the retinal vasculature to maintain a steady supply of oxygen. Although the vascular reactivity response to hyperoxia has been extensively studied, most of these studies used a 100% inspired oxygen stimulus. The aim of this study is to explore the relationship between retinal vascular reactivity and incremental changes in hyperoxia during isocapnia, in addition to providing normative data for the retinal hemodynamic response to incremental changes in hyperoxic stimuli during isocapnia.

Method: Twelve healthy, young adults participated in a gas protocol consisting of 4 phases at varying fractional expired oxygen levels (FeO_2): baseline (15%), hyperoxia I (40%), hyperoxia II (65%), and recovery (15%). End-tidal carbon dioxide ($ETCO_2$) was maintained at an isocapnic level (~ 5%) throughout the experiment. Retinal arteriolar diameter, blood velocity, and blood flow were assessed non-invasively using the Canon Laser Blood Flowmeter during each of these phases.

Results: Repeated measures ANOVA showed that there were significant influences of incremental changes in FeO_2 on arteriolar diameter ($p < 0.0001$), blood velocity ($p < 0.0001$), and blood flow ($p < 0.0001$) in the retina. Paired t-tests of these retinal hemodynamic parameters during each phase in the gas sequence showed they were significantly different ($p < 0.05$) from each other, with the exception of baseline and recovery values. Incremental increases in FeO_2 caused a linear decrease in group mean

arteriolar diameter ($R^2 = 1$, $p = 0.002$), group mean blood velocity ($R^2 = 0.9968$, $p = 0.04$), and group mean blood flow ($R^2 = 0.9982$, $p= 0.03$).

Conclusions: Isocapnic hyperoxia elicits vasoconstriction and the reduction of retinal arteriolar blood flow in a dose-dependent manner over the range of FeO_2 explored in this study.

4.1.1 Introduction

Vascular reactivity is defined as the magnitude of change of hemodynamic parameters in response to provocative stimuli, such as the manipulation of the partial pressures of O_2 or CO_2 (pO_2 or pCO_2) in inspired gases. Retinal blood flow varies inversely with the pO_2 to maintain tissue oxygenation at a constant level, and also varies directly with the pCO_2. Oxygen supply to the retina during hyperoxia is regulated by vasoconstriction[101], which is predominantly mediated by the release of endothelin-1 by vascular endothelial cells[57].

An effective method of delivering a hyperoxic stimulus while maintaining stable isocapnia through a sequential re-breathing circuit[102] was used to evaluate the retinal vascular effect of approx 95% inspired oxygen in healthy participants [55]. However, inhalation of pure oxygen or oxygen-enriched gas dilutes the blood concentration of carbon dioxide, which exaggerates the vasoconstrictive effect of oxygen in retinal vasculature[112]. Maintaining isocapnia allows the true effect of elevated blood concentration of oxygen to be studied [95]. A computer-controlled gas sequencer, in conjunction with the sequential rebreathing circuit, allows the automated controlled delivery of oxygen through breath-by-breath adjustments to the delivered gas mixture [132].

The comprehensive study of hemodynamics in the human retina requires the use of techniques that allow the non-invasive, quantitative measurement of blood flow. Using the Canon Laser Blood Flowmeter, it is now possible to simultaneously assess retinal vessel diameter and quantify centerline blood velocity using bidirectional laser Doppler velocimetry to derive volumetric retinal blood flow in absolute units, non-invasively. This offers an advantage over previous studies of ocular blood flow and vascular reactivity in the human retina which had technical issues including the assignment of arbitrary units to blood flow or the inability to quantify changes in blood flow in relation to changes in blood vessel diameter[83].

The study described in the previous chapter compared retinal hemodynamic changes to the maximum hyperoxic provocation that can be delivered using a manually-controlled gas delivery system and the computer-controlled gas sequencer. Although there was a >15% difference in FeO_2 during maximum hyperoxic provocation between manually-controlled (85.27 ± 0.29%) and computer-controlled (69.02 ± 2.84%) gas delivery systems, the retinal hemodynamic response from normoxia in terms of arteriolar diameter, blood velocity, and flow were not significantly different. From these results, the nature of vascular reactivity in the human retina in response to systemic hyperoxia is unclear. It could perhaps be an indication that there is a threshold effect, whereby there is a decreased ability of retinal vessels to autoregulate against changes in arterial oxygen tension beyond a certain concentration.

The primary aim of the study is to assess the retinal arteriolar vascular response to incremental increases in inspired O_2 at isocapnia in healthy participants. It is hypothesized that incremental oxygen delivery will result in incremental changes in retinal arteriolar blood flow. The study may provide insight into the rate of change of retinal blood flow relative to changes in FeO_2.

4.2 Materials and Methods

4.2.1 Participants

Fourteen adults were recruited into the study but the data from two were excluded due to poor fixation during imaging and inadequate gas control (ie. Inability to stabilize FeO_2 and $ETCO_2$ during CLBF measurements due to fatigue). Of the12 participants whose data was included in the analysis, there were 6 men and 6 women, ranging in age from 19 to 34 years (mean age 26.2 years, SD ± 4.08). All participants had 20/20 visual acuity or better. Participants were excluded if they had a refractive error of >± 6.00 DS

and /or ± 2.50 DC, ocular disease or disorder including lenticular opacity, and a history of intraocular or refractive surgery in order to avoid light scatter that may interfere with imaging [91]. Additional exclusion criteria included existing or a history of endocrine disease, and systemic disease including respiratory disorders, cardiovascular disease, and hypercholesterolemia. Current cigarette smokers or anyone who had ceased smoking for less than 6 months prior to study participation were also excluded from the study[114]. Participants were asked to abstain from caffeine for 24 hours prior to their involvement in the study[113]. The study received the approval of the University of Waterloo Office of Research Ethics. Informed consent was obtained from each participant after thorough explanation of the nature of the study and its possible consequences, according to the tenets of the Declaration of Helsinki.

4.2.2 Sample Size Rationale

Existing data from our lab shows that retinal blood flowed at a rate of 9.4 μL/min at baseline normoxic conditions (FeO_2 = 15%) and 5.1 μL/min during isocapnic hyperoxia (FeO_2 =85%), with a mean difference of 4.3 μL/min (SD 1.9)[55]. The standardized effect size for each FeO_2 interval was defined as the mean change in retinal blood flow divided by the standard deviation. For the purpose of this study normoxia was defined as 14% FeO_2. Assuming a linear relationship between FeO_2 and retinal blood flow, interpolation of these results estimated the expected blood flow and standardized effect sizes during each defined hyperoxic stimulus as summarized in Table 4-1.

Table 4-1. Expected Blood Flow and Standardized Effect Sizes.

ΔFeO_2	*Δ Retinal Blood Flow*	*Standardized Effect Size*
14% to 40%	-2.0 μL/min	1.0
40% to 65%	-1.3 μL/min	0.7

For a standardized effect size of 1.0, an α-level of 0.05, and a β-level of 0.1, the requisite sample size for statistical significance is n = 11. Since there are two possible randomized sequences in this study, sample size was increased to n = 12 so that each of these sequences could be used randomly but equally.

4.2.3 Pre-data Collection Screening

Prior to data collection, a screening was performed to ensure that each participant met the study criteria. A medical history was taken with questions pertaining to the aforementioned exclusion criteria. Blood pressure and pulse measurements were also taken using an automated sphygomanometer (Omron Digital Blood Pressure Monitor HEM-907, Intellisense^{TM}).

Visual acuity was measured with the Early Treatment of Diabetic Retinopathy Study (ETDRS) logMAR charts.

Prior to CLBF data acquisition, a drop of fluorescein was applied to the cornea to detect corneal abrasions or tear film irregularities that may interfere with CLBF imaging. Ophthalmic drops were used only if study participants reported no known allergies to the drugs. Van Herrick's angle assessment was performed to determine the risk of anterior angle closure, prior to the use of mydriatic drops. Once it was determined that mydriasis was safe (ie. cornea to chamber ratio > 1:1/2), one drop of 1% Tropicamide was applied to the randomly chosen study eye.

4.2.4 Gas Delivery

The computer-controlled gas delivery system that was described in the previous chapter was used for the study. Briefly, the system incorporates a sequential re-breathing circuit[102] with a computerized end-tidal

gas monitoring system that regulates the flow of O_2, CO_2, and N_2 to the participant on a breath-by-breath basis, according to pre-specified $PetO_2$ and $PetCO_2$ targets[116]. For this study, the computer-controlled system was favoured over the manually-controlled system for several reasons. Firstly, as demonstrated in the previous study, the computer-controlled system normalizes $PetCO_2$ across participants and over time. Secondly, the computer-controlled system more tightly regulated $PetO_2$ during hyperoxia, reducing the variation in retinal hemodynamic measurements between participants. In addition, the computer-controlled system was designed to clamp CO_2 and O_2 independently of each other, irrespective of the ventilation rate, which can be affected by prolonged hyperoxic exposure. Due to this specific targeting, square waveform patterns can be achieved during the gas transitions, allowing gas targets to be met in a timely fashion [132]. Furthermore, the hyperoxic stimulus was limited to maximal FeO_2 levels for each participant and cannot be specifically targeted. As the aim of the study was to provide normative retinal hemodynamic data for incremental changes in FeO_2, the computer-controlled system was the appropriate choice.

4.2.5 Retinal Hemodynamic Measurements

Retinal hemodynamic measurements were taken noninvasively with the Canon Laser Blood Flowmeter (CLBF). A measurement site was chosen approximately one disc diameter from the optic nerve head in the superior temporal arteriole. The CLBF simultaneously measures vessel diameters and red blood cell velocity through the measurement site and derives volumetric blood flow. Since these calculations assume Poiseuille's flow (non-turbulent flow) and a circular vessel profile, measurement sites were chosen in a relatively straight segment of the arteriole that was free of bifurcations.

4.2.6 General Protocol

Participants were fitted with a face mask and a gas delivery system comprising a sequential rebreathing circuit through which they breathed a controlled mixture of gases. The sequential rebreathing circuit consisted of fresh and rebreathed gas reservoirs. A transparent medical film dressing (3M™ Tegaderm™, St. Paul, MN) was used to secure the mask and to create an airtight seal around the face.

A gas sequence consisting of four phases – baseline, hyperoxia I, hyperoxia II, and recovery – was used to stimulate retinal hemodynamic changes. End-tidal CO_2 was targeted at approximately 5% and maintained throughout the phases. The FeO_2 levels that were targeted in each phase are summarized in Table 4-2.

Table 4-2. FeO_2 Targets Defined in the Study

Phase	*FeO_2 Target*
Baseline	15%
Hyperoxia I	40%
Hyperoxia II	65%
Recovery	15%

Participants were randomly assigned to one of two sequences (Figure 4-1), which differed only in the order in which the Hyperoxia I and Hyperoxia II phases were administered, and were masked to which sequence they were given. Vasoconstriction has been shown to persist within 10 minutes after cessation of a hyperoxic stimulus[133], likely due to the relatively long half-life of ET-1[57;58;134]. The design of this study negates the potential influence of an order effect by randomizing the order of the hyperoxia phases, which may vary in the persistence of vasoconstriction after removal of the hyperoxic stimulus due to the

differences in FeO_2 elevation. A stabilization period (10 minutes) was allowed after each hyperoxic phase before hemodynamic measurements to further prevent this influence.

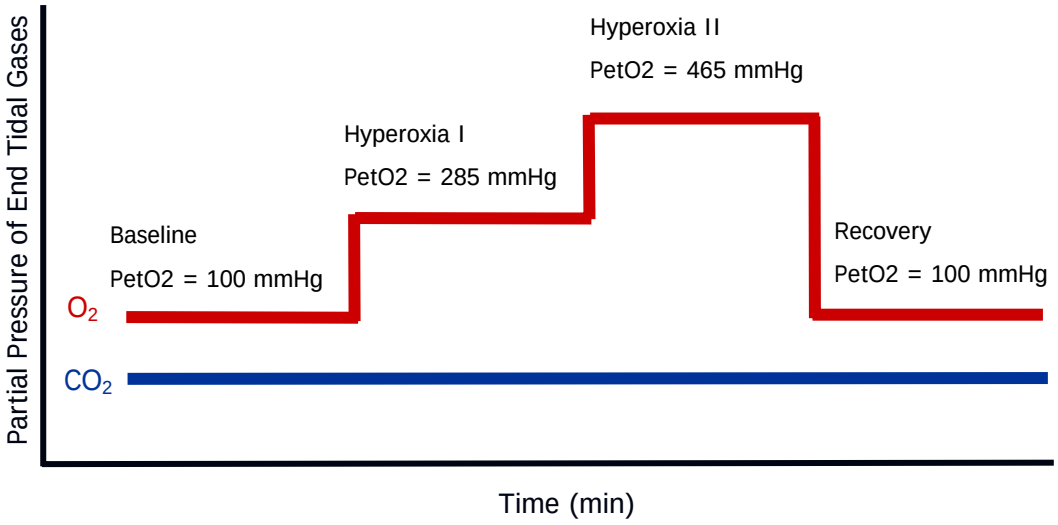
Partial Pressure of End Tidal Gases
Hyperoxia II
PetO2 = 465 mmHg
Hyperoxia I
PetO2 = 285 mmHg
Baseline
PetO2 = 100 mmHg
Recovery
PetO2 = 100 mmHg
O2
CO2
Time (min)

A

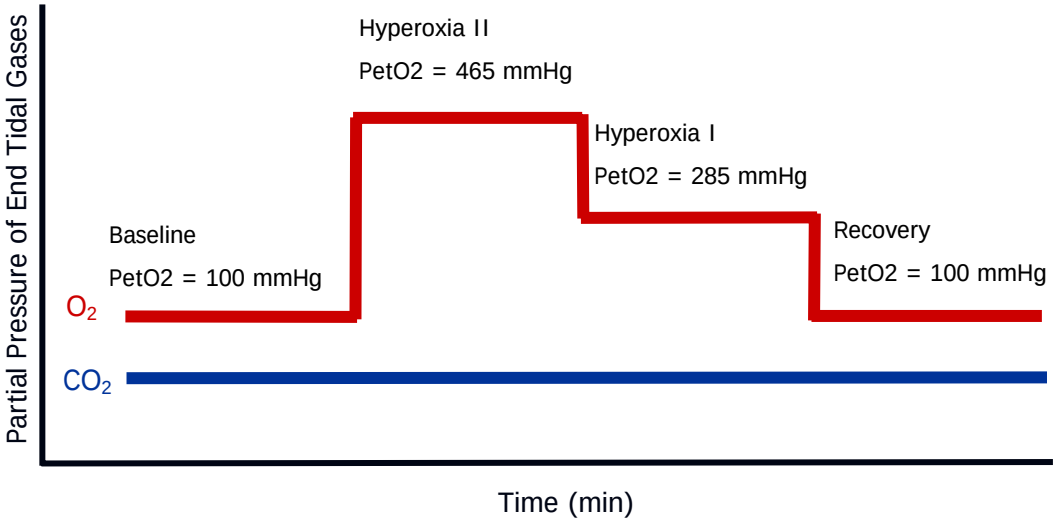
Partial Pressure of End Tidal Gases
Hyperoxia II
PetO2 = 465 mmHg
Hyperoxia I
PetO2 = 285 mmHg
Baseline
PetO2 = 100 mmHg
Recovery
PetO2 = 100 mmHg
O2
CO2
Time (min)

B

Figure 4-1. Gas Sequence for Study Protocol.
Hyperoxia I and II were presented in random order such that each participant received either the treatment represented in A or B. Isocapnia is maintained throughout the protocol, as indicated by the flat blue line (CO_2). The red line (O_2) reflects changes in FeO_2 which was targeted at 40% and 65% for the Hyperoxia I and II phases, respectively and 14% for Baseline and Recovery phases. FeO_2 and $ETCO_2$ are simply expressed as percentages of $PetO_2$ and $PetCO_2$ over atmospheric pressure (760 mmHg).

Before commencing data collection, participants were asked to rest for at least 20 minutes to ensure that all metabolic parameters were representative of baseline, resting conditions. Once the gas mask was attached, participants breathed air that was delivered through the mask until their tidal volumes of CO_2 and O_2 were stabilized, upon which the gas sequence was initiated. $PetCO_2$ and $PetO_2$ levels were allowed to stabilize at the start of each phase before CLBF measurements were made. More importantly, if the particular phase was preceded by one with a higher targeted $PetO_2$ a period of at least 10 minutes would be allowed, as long as it did not affect the participant's reported comfort. The additional time was required since it was found in a previous study in our lab and others that hyperoxic provocation resulted in a persistent vasoconstriction up to 10 minutes after cessation of the stimulus (unpublished data, paper in submission)[101;133]. During each phase, 6 CLBF measurements were taken at 1 minute intervals.

4.2.7 Data Analysis

4.2.7.1 Gas Data

End-tidal gas parameters were recorded directly by a computer-controlled gas delivery system on a breath-by-breath basis. $PetO_2$ and $PetCO_2$ were reported in mmHg, and were converted to FeO_2 and $ETCO_2$ which are reported as a percentage of the atmospheric pressure.

Upon plotting FeO_2 and $ETCO_2$ against time (min), any values derived during the transition between normoxic and hyperoxic phases were excluded. Data points lying outside the 10^{th} and 90^{th} percentiles (ie. 3 SDs from the mean) of each phase were excluded as outliers, and were likely the result of misinterpretation of the tidal waveforms by the gas monitor.

4.2.7.2 CLBF Data

A post-acquisition analysis of the velocity waveforms were performed using a standardized protocol to remove aberrant waveforms affected by eye movements, tear film breakup, or improper tracking of the measurement laser. Velocity waveforms were accepted if there was a minimum of one complete cardiac cycle which was not adversely affected by major eye movements, ie. more than 50 μm in each direction.

4.2.7.3 Statistical Analysis

Differences in end-tidal gas parameters ($ETCO_2$ and FeO_2) for each phase (baseline, hyperoxia, and recovery) were analyzed using repeated measures ANOVA (reANOVA) Similarly, differences in retinal hemodynamic parameters (blood vessel diameter, blood velocity, and blood flow) were analyzed using reANOVA for each phase. Regression analysis was performed to explore the relationship between FeO_2 and group mean hemodynamic measurements.

4.3 Results

4.3.1 End-Tidal Gas Parameters

Repeated measures ANOVA showed that $ETCO_2$ was significantly different between subjects ($p < 0.0001$). However, there was no significant effect of the phases in the gas sequence ($p = 0.3271$), indicating that within subjects, $ETCO_2$ levels remained constant throughout the protocol.

For FeO_2, reANOVA showed that differences between subjects was not significant ($p = 0.4559$). The effect of the phases in the gas sequence was found to be significant ($p < 0.0001$). *Post hoc* t-tests (LSD) showed that FeO_2 was significantly different between each pair of phases ($p < 0.05$), except for the comparison between baseline and recovery FeO_2 levels. Mean FeO_2 at baseline was 14.24 ± 0.34%, and each successive phase increased linearly by 25% increments to 39.74 ± 0.34% and 64.65 ±1.47% for hyperoxia I and hyperoxia II, respectively. The means and SDs values for $ETCO_2$ and FeO_2 levels are summarized in Table 4-3 and boxplots are show in Table 4-2 and Table 4-3 .

Table 4-3. Summary of End-Tidal Gas Parameters.

	Baseline	***Hyperoxia I***	***Hyperoxia II***	***Recovery***
$ETCO_2$	5.59 ± 0.62	5.54 ± 0.57	5.52 ± 0.54	5.62 ± 0.58
FeO_2	14.24 ± 0.34	39.74 ± 0.34	64.65 ± 1.47	14.30 ± 0.30

Values expressed in mean % ± SD (n = 12).

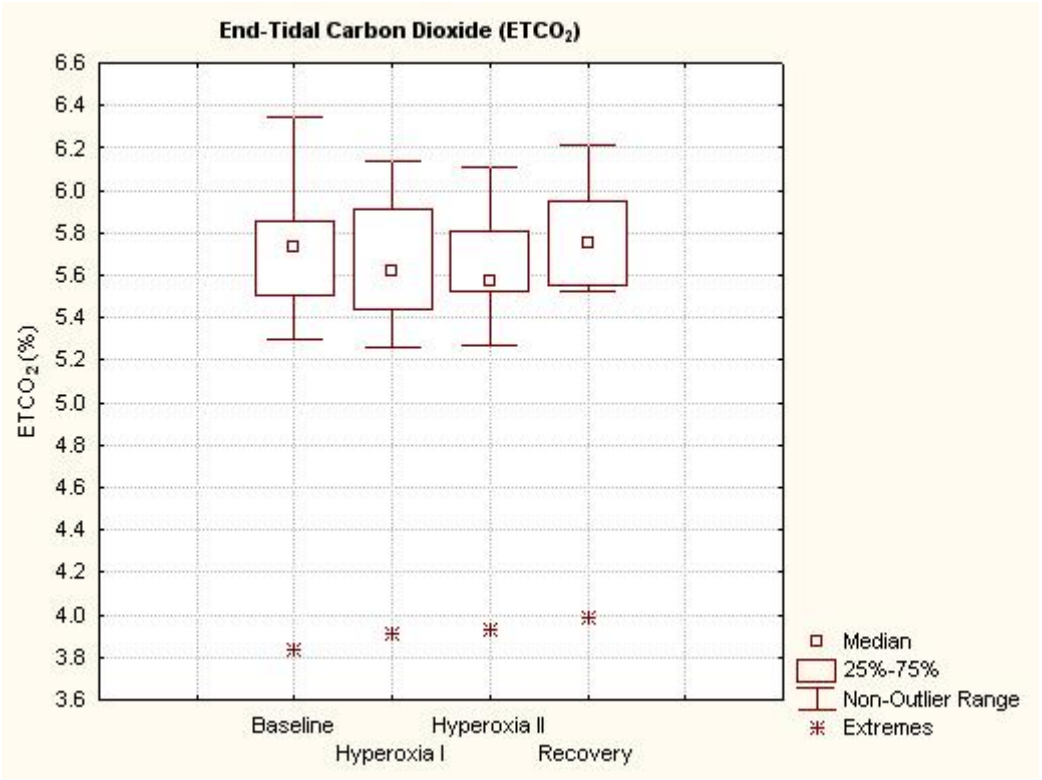

Figure 4-2. Boxplot of $ETCO_2$.

The non-outlier range (whiskers) is defined as 1.5H below the 25th percentile or above the 75th percentile, where H is the height of the box or the interquartile range. Extreme outliers are denoted by asterisks (*), indicating that the values fall 3H below the 25th percentile or above the 75th percentile.

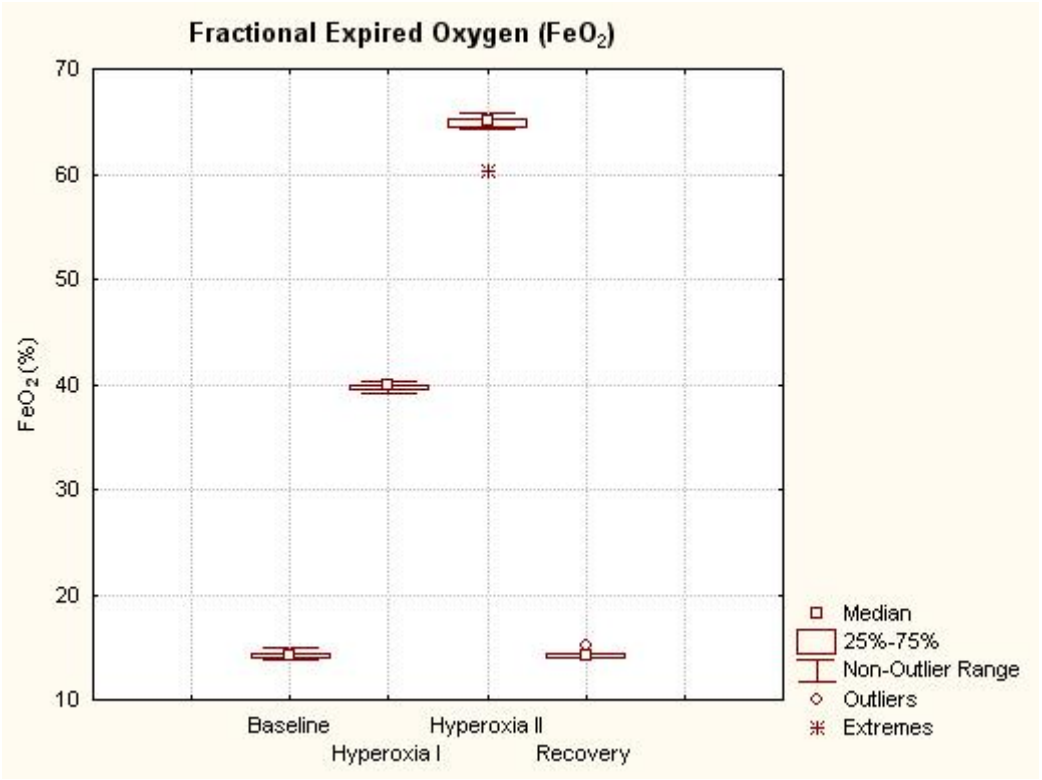

Figure 4-3. Boxplot of FeO_2.

The non-outlier range (whiskers) is defined as 1.5H below the 25th percentile or above the 75th percentile, where H is the height of the box or the interquartile range. Outliers are values that lie beyond the non-outlier range and are denoted by open circles (○).Extreme outliers are denoted by asterisks (*), indicating that the values fall 3H below the 25th percentile or above the 75th percentile.

4.3.2 Retinal Hemodynamics

Relative to baseline, a reduction in arteriolar diameter, blood velocity, and blood flow was observed during hyperoxia I and hyperoxia II. Difference in each of the retinal hemodynamic parameters between participants was significantly different ($p < 0.0001$ for diameter, velocity, and flow). The effect of the gas phases on each of the retinal hemodynamic parameters was also significant ($p < 0.0001$ for diameter, velocity, and flow). The group means and standard deviations for arteriolar diameter, blood velocity, and blood flow by gas phases (baseline, hyperoxia I, hyperoxia II, and recovery) are reported in Table 4-4. Boxplots for each of these parameters are shown in Figure 4-4, Figure 4-5, and Figure 4-6.

Table 4-4. Summary of Retinal Hemodynamic Parameters.

	Baseline	***Hyperoxia I***	***Hyperoxia II***	***Recovery***
Arteriolar Diameter (μm)	110.2 ± 11.1	105.9 ± 13.2	101.6 ± 12.0	110.6 ± 10.8
Blood Velocity (mm/s)	33.1 ± 9.9	28.6 ± 7.8	23.4 ± 5.1	32.1 ± 8.1
Blood Flow (μL/min)	9.8 ± 4.3	7.9 ± 3.9	5.8 ± 2.2	9.5 ± 3.6

Values expressed as mean ± SD (n = 12).

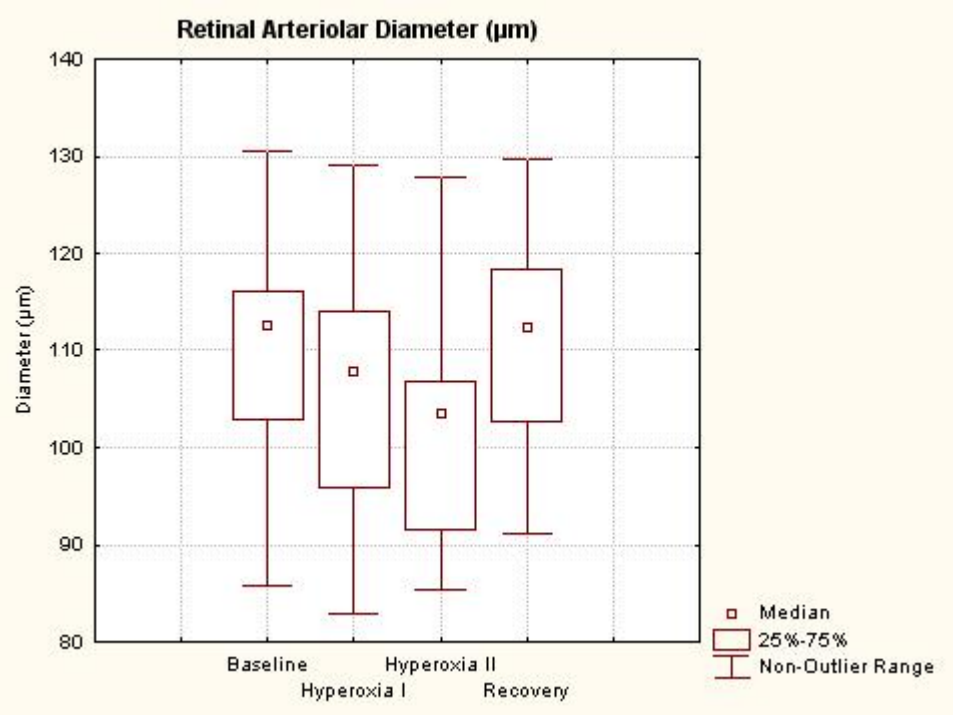

Figure 4-4. Boxplot of Retinal Arteriolar Diameter.

The non-outlier range (whiskers) is defined as 1.5H below the 25th percentile or above the 75th percentile, where H is the height of the box or the interquartile range.

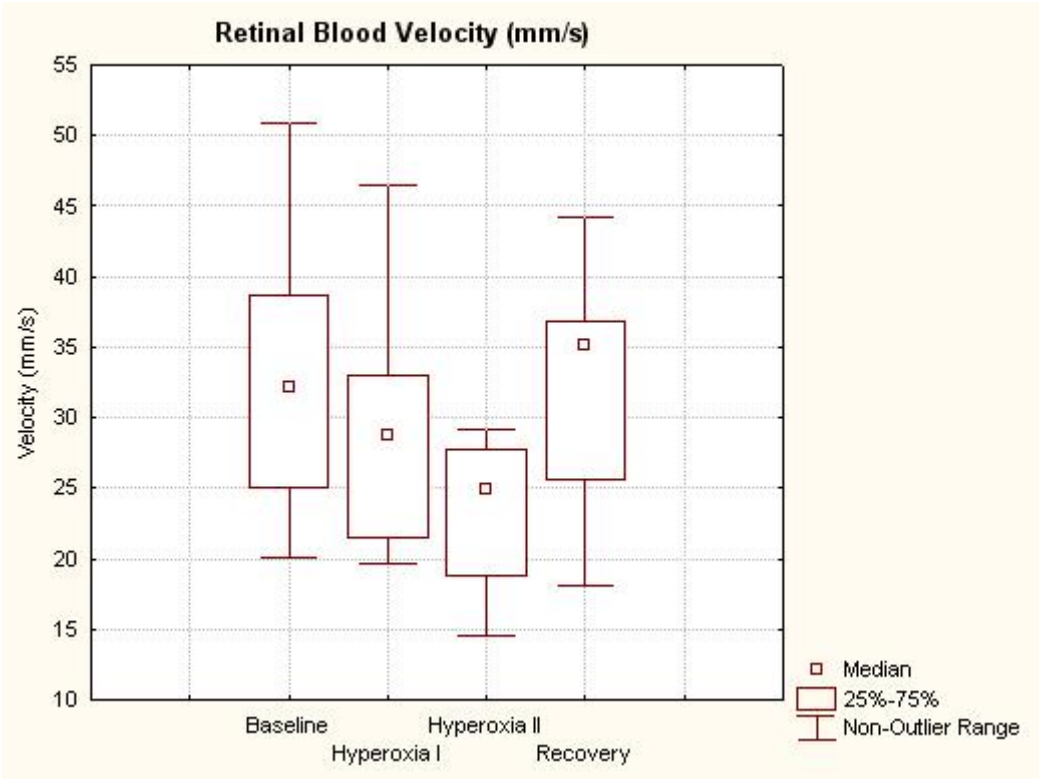

Figure 4-5. Boxplot of Retinal Blood Velocity.

The non-outlier range (whiskers) is defined as 1.5H below the 25th percentile or above the 75th percentile, where H is the height of the box or the interquartile range.

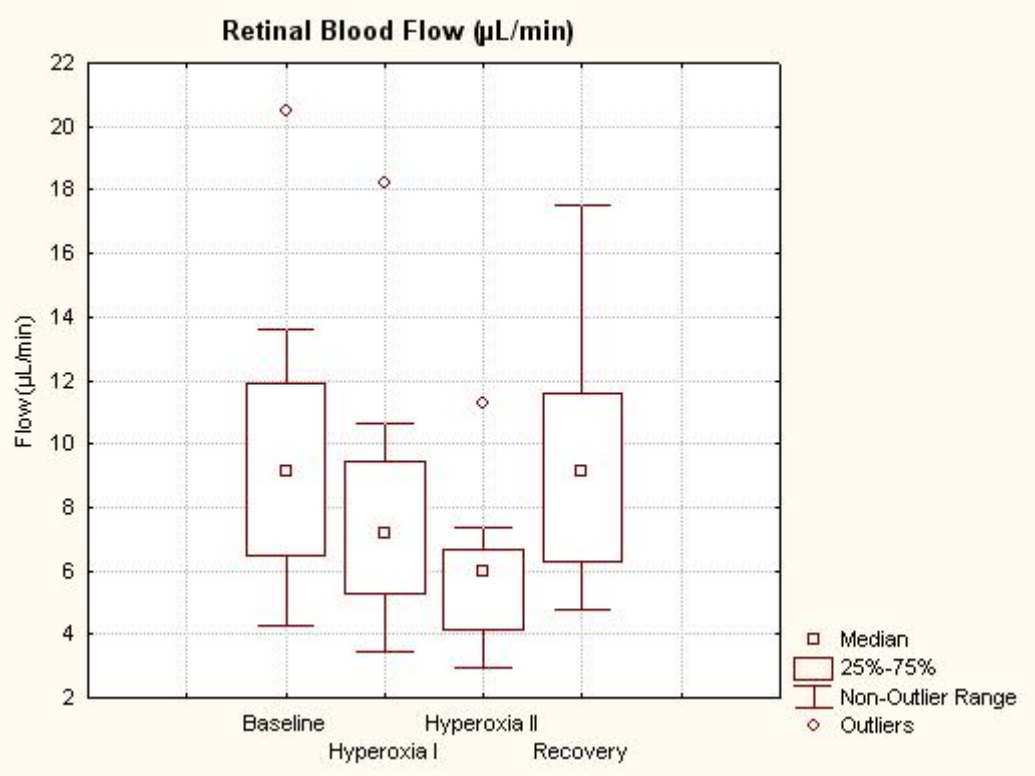

Figure 4-6. Boxplot of Retinal Blood Flow.

The non-outlier range (whiskers) is defined as 1.5H below the 25th percentile or above the 75th percentile, where H is the height of the box or the interquartile range. Outliers are values that lie beyond the non-outlier range and are denoted by open circles (○).

Retinal arteriolar diameter decreased with incremental hyperoxia. A pairwise comparison of the gas phases using a t-test showed that with the exception of the baseline to recovery comparison, all other pairs of phases were significantly different in terms of retinal arteriolar diameter ($p < 0.05$). Hyperoxia II produced a greater reduction in diameter relative to baseline (-7.82%) than hyperoxia I (-3.94%).

A similar pattern of reduction was observed in the velocity of red blood cells traveling through the sampling site. With the exception of the baseline to recovery comparison, pairwise comparisons of velocity during each gas phase using the t-test showed that each phase was significantly different ($p < 0.05$). Relative to baseline, hyperoxia I and hyperoxia II produced changes in velocity of -13.3% and -29.3%, respectively.

Retinal blood flow followed the same pattern of reduction in the face of increases in inspired oxygen stimulus. All pairwise comparisons using t-tests of retinal blood flow during each pair of gas phases were significantly different ($p < 0.05$), although baseline and recovery were the same. Incremental increases in FeO_2 produced reductions in flow such that hyperoxia I changed by -1.8% and hyperoxia changed by -2.1%, relative to baseline.

4.3.3 Correlation Between Group Mean FeO_2 and Group Mean Retinal Hemodynamic Parameters

When group means of retinal arteriolar diameter, blood velocity, and blood flow were each plotted against the group mean of FeO_2 (for all phases minus recovery), each of the retinal hemodynamic parameters were significantly varied inversely with changes in FeO_2. Diameter ($R^2 = 1$, $p = 0.002$), velocity ($R^2 = 0.9968$, $p = 0.04$), and flow ($R^2 = 0.9982$, $p = 0.03$) had strong linear correlations with FeO_2. Data from individual participants showed similarly strong linear correlations in the majority of cases.

With FeO_2 as the independent variable and retinal arteriolar diameter (RAD), retinal blood velocity (RBV), and retinal blood flow (RBF) as dependent variables, retinal hemodynamics are generally related to FeO_2 by the following equations, and illustrated in Figure 4-7. Despite differences in R^2 values, the equation from the linear regressions remain the same whether they include only the group mean data or the individual data.

$$RAD = -0.17\ FeO_2 + 113$$

$$RBV = -0.19\ FeO_2 + 36$$

$$RBF = -0.08\ FeO_2 + 11$$

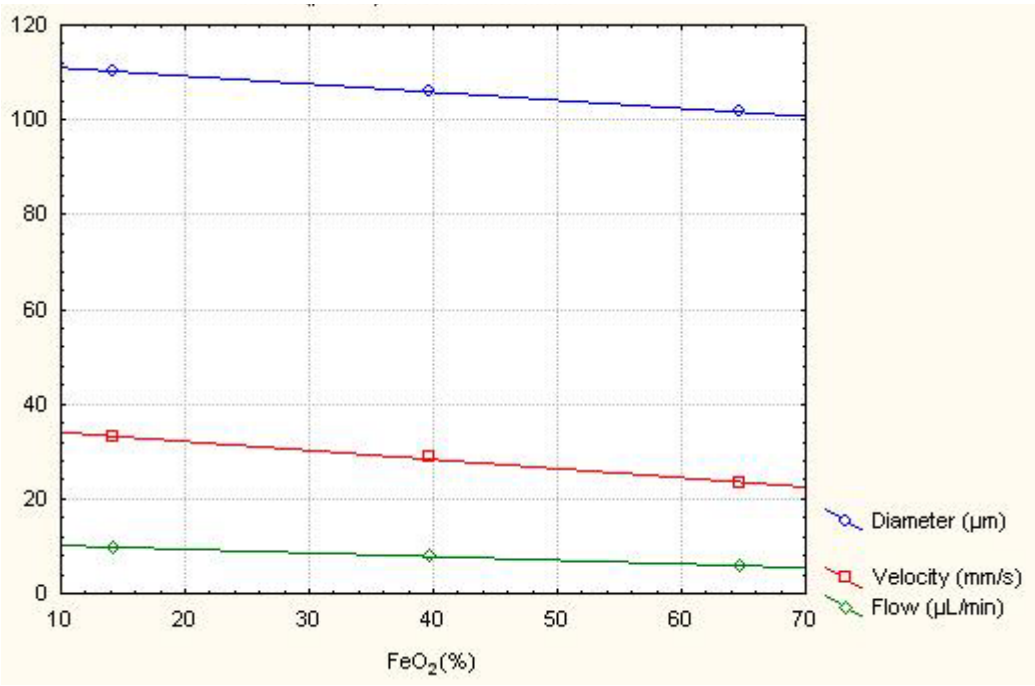

Figure 4-7. Linear Regression of Group Mean Retinal Hemodynamic Parameters Against Changes in FeO_2 in the range from 15% to 65%.

4.4 Discussion

The primary aim of this study was to define the retinal hemodynamic response to incremental changes in systemic hyperoxia during isocapnia. The data strongly demonstrates that retinal arteriolar diameter, blood velocity, and blood flow varies inversely and linearly with incremental changes in FeO_2.

It is generally accepted that incremental changes in end-tidal partial pressures of O_2 and CO_2 correlate well to systemic arterial O_2 and CO_2 tension which varies by the proximity of the peripheral sampling site to the lungs [112]. Expired gases (FeO_2 and $ETCO_2$) can thus be validly used as surrogate measures of the partial pressures of O_2 and CO_2 in arterial blood. Incremental changes in end-tidal partial pressures of O_2 and CO_2 are also believed to more closely reflect the metabolic rate than inspired gas. In this study, $ETCO_2$ was maintained throughout the experimental protocol within subjects, so changes in retinal arteriolar diameter, blood velocity, and blood flow can be attributed to changes in FeO_2. Although baseline $ETCO_2$ varied significantly between participants, it is likely that the high degree of control of end-tidal gases within subjects amplified the individual variation between participants. On average, $ETCO_2$ was maintained at close to 5%, a level which is considered normocapnic.

Based on the slopes of the linear regressions, for every 1% increase in FeO_2 within the limits of this study (~ 15% to 65% FeO_2), retinal arteriolar diameter decreased by approximately 0.17 μm, velocity decreased by approximately 0.19 mm/s, and flow decreased by approximately 0.08 μL/min. Based on the mean retinal hemodynamic measurements at normoxia, this represents a 0.15% decrease in arteriolar diameter, a 0.57% decrease in blood velocity, and 0.82% decrease in blood flow. Increases in FeO_2 have the greatest effect on blood flow, due to the compound effect of decreases in both vessel diameter and centerline blood velocity. This is not surprising because according to Poiseuille's law of non-turbulent flow (which is assumed in the small blood vessels measured by the CLBF), the fourth power of the radius

is directly related to the rate of flow. Small changes in diameter would thus result in greater changes in flow.

Regression analysis of the group means of each of the hemodynamic parameters across baseline (14.24 ± 0.34% FeO_2), hyperoxia I (39.74 ± 0.34% FeO_2), and hyperoxia II (64.65 ± 1.47% FeO_2) yielded results that indicated nearly perfect linear correlation between FeO_2 and arteriolar diameter ($R^2 = 1$, $p = 0.002$)), blood velocity ($R^2 = 0.9968$, $p = 0.04$), and blood flow ($R^2 = 0.9982$, $p = 0.03$). Since baseline and recovery phases were not significantly different for gas nor hemodynamic parameters, values from the recovery phase were excluded from the regression analysis to avoid doubling the sample points for the normoxic condition. When regression analysis was performed using data from the individual participants (rather than a group mean), similar linear relationships were found. Given this evidence, we have demonstrated that retinal blood flow is reduced in a linear manner in the presence of systemic hyperoxia (over the range of 15 – 65% FeO_2) and isocapnia, due to the linear reduction of arteriolar diameter and blood velocity.

A recent study in our lab has identified a persistent vasoconstrictive effect of hyperoxia *within* 10 minutes after the cessation of the stimulus[133]. Although it was beyond the scope of that particular study to determine the underlying cause, it was speculated that endothelin-1 (ET-1), a potent endothelium-derived vasoconstricting agent which mediates hyperoxia-induced vasoconstriction was responsible. Studies to date suggest that the half-life of ET-1 could be as short as 1.4 to 3.6 minutes, or as long as 35 minutes[134]. It has also been suggested that persistent vasoconstriction following pronounced hyperoxia (ie. approximately 94% inspired O_2) could be a consequence of oxidative damage at the level of the retinal vasculature[63].

Several precautionary measures were taken in order to avoid the confounding effects of persistent hyperoxia-induced retinal vasoconstriction in this study. First, hyperoxia I (target FeO_2 = 40%) and hyperoxia II (target FeO_2 = 65%) phases were administered in random order. Furthermore, at the transition between phases, when FeO_2 was either raised or lowered, a 10 minute period of breathing was allowed before CLBF measurements were taken – although in some cases, this time period had to be abbreviated depending on the participant's reported discomfort with the procedure. Since the recovery values for arteriolar diameter, velocity, and flow were not significantly different from the baseline values, it is reasonable to conclude that the hemodynamic response during each phase is independent of other phases in the gas protocol.

Although it might have been informative to include more levels of hyperoxia in the study protocol, this was limited by the fact that subjects could not comfortably tolerate the amount of time required to do so. However, given the high degree of correlation as indicated by the R^2 values, it is unlikely that inserting more phases within the existing FeO_2 intervals would change this relationship. The FeO_2 levels chosen for this study encompasses a range between normoxia and a level that approaches the upper limit for the majority of participants for this particular method of hyperoxia induction. In the study presented in Chapter 3, the same gas delivery method (computer-controlled) produced a level of hyperoxia of 69.02 ± 2.84% FeO_2, although several of the participants could not reach the 70% FeO_2 target. The hyperoxia protocol for the manually-controlled gas delivery system was designed to target the maximum FeO_2 in each participant, achieving a group mean of 85.27 ± 0.29% FeO_2. This study was originally intended only for the comparison of the retinal hemodynamic response to a hyperoxic stimulus administered using two different gas delivery systems. However, since FeO_2 during hyperoxia was significantly different when comparing the two systems hemodynamic data from this study was used as additional coordinates for regression analysis to explore the relationship between FeO_2 and hemodynamics in the 65% to 85%,

given that linearity was established in the 15% to 65% FeO_2 range. When these additional coordinates were included in the regression analysis, the linear relationship between FeO_2 and the retinal hemodynamic response was preserved (Figure 4-8). The correlations for arteriolar diameter ($R^2 = 0.9314$), blood velocity ($R^2 = 0.9980$), and blood flow ($R^2 = 0.9909$) were very strong and comparable to the regression using only the coordinates of the current study. The slopes and intercepts for each remained the same for the blood velocity response, and remained very similar for arteriolar diameter, and blood flow, as shown in the equations below.

$$RAD = -0.13\ FeO_2 + 111$$

$$RBV = -0.19\ FeO_2 + 36$$

$$RBF = -0.07\ FeO_2 + 11$$

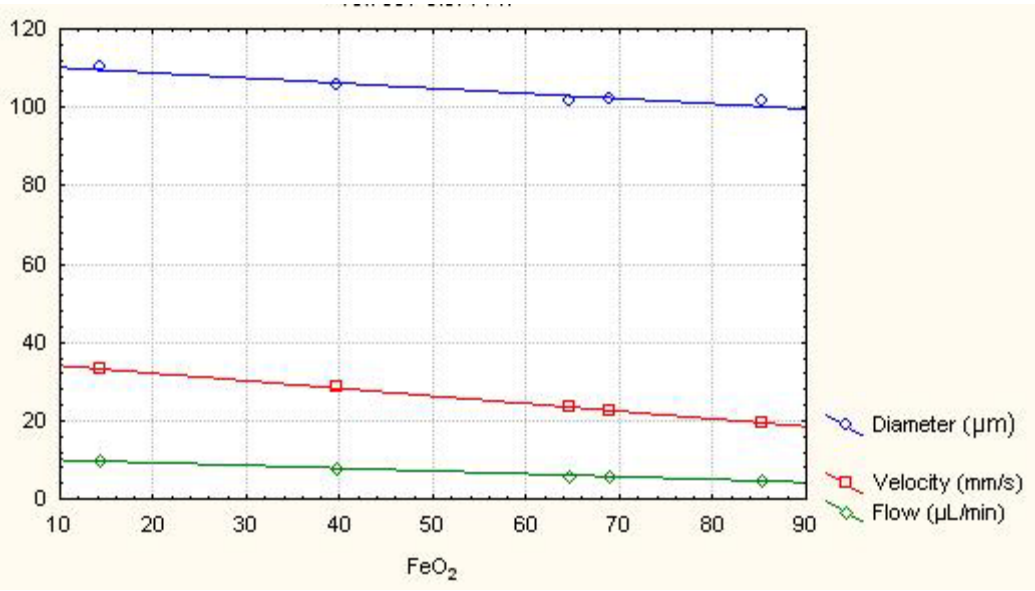

Figure 4-8 Linear Regression of Group Mean Retinal Hemodynamic Parameters Against Changes in FeO_2 in the range from 15% to 85%.

Since regression analysis strongly suggests that linearity between FeO_2 and arteriolar hemodynamics is maintained, then it follows that the retinal hemodynamic parameters were each reduced at the same rate when FeO_2 rises in the 65-85% range as it did between the 15-65% range. This finding is interesting in light of the fact that retinal arteriolar diameter, blood flow, and blood velocity at 70% and 85% FeO_2 were not significantly different. Prior to the current study which investigated incremental changes in FeO_2, the results might have suggested that the hemodynamic response reached a plateau during pronounced systemic hyperoxia. The current evidence would suggest that this does not occur within the studied range. The previous study (Chapter 3) showed a trend of a greater reduction from baseline of all the hemodynamic parameters using the manually-controlled gas delivery system because of a higher group mean FeO_2, even if this difference was not statistically different. It is likely that a statistical difference was not found because the interval between the two hyperoxic phases was much smaller than the interval between the hyperoxic and normoxic phases. The previous study needs to be interpreted with caution because of the relatively small sample size used.

Based on this evidence, it is reasonable to conclude that when systemic oxygen tension varies between 15% (normoxia) and 85% FeO_2, retinal arteriolar diameter, blood velocity, and blood flow are related to FeO_2 inversely and linearly when $ETCO_2$ is maintained at a normocapnic level. We acknowledge that the limitations of this *post hoc* combination of data from the two studies. A different gas delivery system was used to attain the data during the highest level of hyperoxia. Furthermore, the data was collected under different circumstances, and on a different group of participants (although the participants from both studies met the same inclusion criteria). The studies were also different in sample size, making the data imbalanced. This suggests a *theoretical* linear relationship within the 15-85% FeO_2 range, and provides a basis for further study. A plateau effect at FeO_2 levels that surpasses the range studied here cannot be

ruled out completely. However, with the available gas delivery techniques, it is not possible to study the retinal hemodynamic response at higher FeO_2 levels.

To the best of our knowledge, no other group has investigated the effect of incremental hyperoxia during isocapnia on retinal vascular reactivity. In most studies, O_2 status changes are stimulated by breathing air to 100% O_2[53;70;93-101]; hence, a curvilinear relationship between FeO_2 and retinal hemodynamics cannot be excluded. Other studies have reported graded changes in retinal hemodynamic parameters with graded increases of inhaled O_2[98;100] in a linear manner from hypoxic to hyperoxic ranges[98], but did not employ gas delivery techniques that could regulate gas exchange to standardized systemic pO_2 and pCO_2 conditions between subjects [98;100]. Isocapnia was not maintained[98;100], and even deliberately altered to simultaneously induce hypercarbia[100]. No surrogate measures of arterial O_2 and CO_2 tension were reported to reflect the systemic response to these provocations in some cases[98]. Previous studies induced changes in FeO_2 by breathing gases consisting of a range from 85% to 100% O_2 but induced further changes in vascular reactivity by simultaneously varying CO_2[98]. Moreover, retinal arteriolar diameter and retinal blood velocity could not be simultaneously measured using some techniques[100], and blood flow could only be measured in arbitrary units in others[98]. Given that our methodology offers superior control of gas delivery and simultaneous measurement of vessel diameter and blood velocity[89;90], it presents a more accurate representation of the autoregulatory capacity of retinal arterioles to changes in systemic O_2 tension.

From this study, it can be concluded for the first time that there is linear relationship between RBF and FeO_2 in the 15% (normoxia) to 65% during isocapnia. Additional data from the earlier study strongly suggests that the linearity of the response extends up to 85% FeO_2. The focus of further studies should be to assess changes in retinal vascular autoregulatory dysfunction during graded isocapnic hyperoxic

provocation as it may be more relevant in understanding the etiology of retinal diseases with vascular involvement. The gas provocation protocol described in this study could be used to identify subtle changes in vascular reactivity.

Chapter 5
Discussion

Vascular reactivity to hyperoxia is an important area of research as an impaired magnitude of response has been associated with glaucoma[111], and diabetic retinopathy[18]. Past studies have demonstrated a profound vasoconstriction of retinal arterioles during hyperoxic provocation[53;70;93-101]. When stimulated by pure oxygen breathing, systemic hyperoxia results in a decrease in systemic pCO_2 levels or hypocapnia[63;102]. Carbon dioxide is a potent vasodilator which results in increased blood flow to the retina [66;96]. Consequently, the combined effect of hypocapnia and hyperoxia results in a more exaggerated degree of vasoconstriction and decline in blood flow rate in the retinal vasculature[55;102]. Without controlling against decreases in systemic pCO_2 levels during hyperoxia, retinal vascular reactivity against changes in systemic pO_2 cannot be isolated. Maintaining isocapnia between baseline and hyperoxic conditions is a technically complicated matter that has been attempted in a few studies by co-administration of CO_2 or with the use of a sequential rebreathing circuit[55;102]. The reduction of hemodynamic variables relative to baseline during hyperoxia stimulated by the systemic rebreathing circuit was reported to be smaller than previous studies due to the fact that isocapnia was maintained throughout the study protocol[55;102]. Furthermore, administration of a gas stimulus using the sequential rebreathing circuit produced less variability in retinal hemodynamic measurements than other methods, an additional benefit to better stimulus control[55] that should improve the statistical power of the provocation.

Although the sequential rebreathing circuit provided superior control of $ETCO_2$, a surrogate measure of systemic pCO_2, it is not capable of providing precise incremental changes in FeO_2. The first study (Chapter 3) comparing the magnitude and variability of the retinal hemodynamic response to isocapnic

hyperoxia induced by the manually-operated sequential rebreathing system to the computer-controlled gas delivery system confirmed this point. The quartile range for FeO_2 during hyperoxia was 10.25% for manually-operated system compared to 0.33% for the computer-controlled system. Furthermore, the COV for FeO_2 during hyperoxia was higher for the manually-operated system than it was for computer-controlled system, at 6.6% vs. 4.1%, respectively. The hyperoxic FeO_2 values were significantly higher for the manually operated method than the computer-controlled method. The computer-controlled method produced a lower FeO_2 (69.02 ± 2.84%) than the computer-controlled method (85.27 ± 5.61%) because pure O_2 was not used as one of the gas mixtures supplying the computer-controlled system. Baseline values of FeO_2 were not significantly different between the two gas delivery methods. However, variability of normoxia (baseline) FeO_2 values was similarly lower using the computer-controlled system, albeit less pronounced. The quartile ranges were 0.39% vs.0.33%, and the COVs were 1.9% vs. 1.4% for the manual versus computer-controlled systems. Due to the specific targeting of FeO_2, the computer-controlled gas delivery system is capable of standardizing the hyperoxic stimulus across participants within a study while also reducing variability.

Isocapnia was maintained throughout the gas sequence using both methods of gas delivery. Although the $ETCO_2$ levels during hyperoxia were found to be statistically different from baseline and recovery values, the magnitude of this difference (< 1%) was small enough that it would not have caused an appreciable effect in the retinal vasculature. Interestingly, while the computer-controlled gas delivery system is capable of achieving specific $ETCO_2$ targets, lower variability in $ETCO_2$ was observed with the manually-operated system. Although $ETCO_2$ levels were statistically different between the two gas delivery systems, again, the magnitude of the difference in all phases was small (~0.5%) and unlikely to affect retinal vascular reactivity.

Despite the differences in end-tidal gas parameters described here, Chapter 3 suggests that these differences had no significant effect on the magnitude of retinal hemodynamic measurements during each of the conditions in the gas sequence when comparing the two gas delivery systems. Retinal arteriolar diameter, red blood cell velocity, and blood flow were generally reduced during hyperoxia but despite the differences in the FeO_2 levels that were achieved during hyperoxia using the two different methods of gas delivery, no magnitude of response differences were found between the two methods. Retinal hemodynamic measurements were not significantly different during the baseline and recovery phases, but these results were expected since differences between the two systems during these phases were less than 1% FeO_2. However, the interpretation of the results needs to take into account inherent limitations associated with the relatively small sample size, especially in relation to the equivalence of the magnitude of the vascular reactivity response between gas delivery systems.

Importantly, although the magnitude of retinal hemodynamic measurements was the same between the gas delivery methods, variability was reduced with the computer-controlled method as demonstrated by lower COVs for the majority of conditions. Reduced variability in retinal hemodynamic measurements reflect the better control of FeO_2 levels. The computer-controlled gas delivery system offers the additional advantage of achieving square-wave transitions between baseline and hyperoxia (up to almost 70% FeO_2) while preventing drifts in $ETCO_2$ levels [132]. In contrast, transitions between baseline and hyperoxia are more gradual with the manually-operated system with transient drifts in $ETCO_2$. Without a computerized system that specifically targets FeO_2 and $ETCO_2$ levels, the manually-operated system relies strictly on sequential rebreathing to attain the targets. Square-wave transitions between baseline and hyperoxia phases offer two advantages. Firstly, the targeted end-tidal gas levels can be reached more quickly so experiments can be carried out more efficiently without compromising the comfort and safety of the participant. Secondly, shorter transitions between phases ensure that the conditions under which

hemodynamic measurements are made are more consistent between subjects by negating the impact of gas delivery time on speed of the retinal vascular reactivity response. This suggests that more reliable hemodynamic data can be acquired when hyperoxia is induced using the computer-controlled gas delivery system than with the manually-operated gas delivery system.

Given the technical advantages of using the computer-controlled gas delivery system identified in Chapter 3, this device was selected for the investigation of retinal vascular reactivity to incremental changes in hyperoxia in Chapter 4. As demonstrated in Chapter 3, improved end-tidal gas control resulted in reduced variability of retinal hemodynamic parameters. Reduced variability translates into greater sensitivity for detecting differences or changes, hence, requiring a smaller sample size to achieve adequate statistical power. Unlike previous studies of graded hyperoxia, $ETCO_2$ was controlled throughout the protocol for the first time. This was made possible by the control of $ETCO_2$ independently of FeO_2, and *vice versa*, and independent of minute ventilation of individual participants. The computer-controlled gas delivery system also allowed for the precise incremental administration of hyperoxia without interruption. With isocapnia maintained throughout the protocol, the influence of incremental changes in systemic pO_2 (consisting of 15%, 45%, and 65% FeO_2) on vascular reactivity was isolated.

In the range that was studied in Chapter 4, retinal arteriolar diameter, blood velocity, and blood flow differed significantly with changes FeO_2. This shows that smaller changes in FeO_2 can indeed elicit a detectable response in vascular reactivity using a relatively small sample size (n = 12). The study also establishes the linearity of the relationship between each of the retinal hemodynamic measurements and FeO_2. The correlation is very strong for all parameters. Incremental increases in FeO_2 caused a linear decrease in group mean arteriolar diameter ($R^2 = 1$, $p = 0.002$), group mean blood velocity ($R^2 = 0.9968$, $p = 0.04$), and group mean blood flow ($R^2 = 0.9982$, $p= 0.03$) within the 15% to 65% FeO_2 range. Although

it would have been useful to include more increments of FeO_2 in the study design, only four phases representing three different FeO_2 levels were investigated, since most participants could not comfortably tolerate a longer experiment. Given the strength of the correlation, it is unlikely that additional increments would change this relationship. Unique to this study, incremental changes excludes the possibility that the inverse relationship between FeO_2 and retinal hemodynamic parameters is curvilinear in nature. In the interest of exploring this relationship further, data from Chapter 3 was included in a separate regression analysis, such that retinal hemodynamic parameters measured at 70% and 85% FeO_2 were also included. When this data was included, the relationship was still unequivocally linear for retinal arteriolar diameter ($R^2 = 0.9314$), blood velocity ($R^2 = 0.9980$), and blood flow ($R^2 = 0.9909$). While regression analysis clearly shows that the relationship between FeO_2 and retinal hemodynamics is linear for the range 15 to 85% FeO_2, this conflicts with the finding that retinal hemodynamic measurements were not significantly different between 70% (manually-operated) and 85% (computer-controlled) FeO_2. The fact that retinal hemodynamic measurements were found to be the same at 70% and 85% FeO_2 could be interpreted in two ways: 1) that there is possibly a plateau effect at the upper hyperoxic limits, or 2) that linearity is maintained at the upper hyperoxic limits the study failed to find a significant difference because of sample size limitations. The second interpretation would agree with an earlier report, but that study was limited by the fact that end-tidal gases were not measured so it was difficult to determine the level of systemic hyperoxia that was elicited by each of the gas stimuli [98]. Furthermore, CO_2 levels were not controlled in this study and confounded the results[98]. However, given that the highest level of hyperoxia was induced by pure O_2 breathing, the study achieved the upper hyperoxic limit and still found a linear relationship. The latter regression analysis as described in 4.4 was performed on data that were collected on different occasions, using different gas delivery methods, and on a different sample of people (though with the same inclusion and exclusion criteria). However, given the strength of the correlation, it is reasonable to state that the relationship of vascular reactivity is linear throughout the 15-85% FeO_2 range. More recent

innovations on the computer-controlled gas delivery system will allow higher FeO_2 targets to be used to confirm these results. This was achieved by altering the compositions of the source gases to include a higher concentration of O_2.

In conclusion, improved control of end-tidal gases using a computer-controlled gas delivery system has reduced the variability of hemodynamic measurements in retinal vascular reactivity studies. This improvement renders the techniques employed here more sensitive to detecting changes or differences in different populations or conditions. This thesis demonstrated for the first time that the inverse relationship between hyperoxia and retinal hemodynamic parameters is linear within the studied range (15%-65% FeO_2) during isocapnia. The isocapnic condition is important so that systemic CO_2 does not confound the effect of systemic O_2. This study on young, healthy adults provides normative data against which future studies on various ocular diseases with vascular etiologies can be compared.

Appendix A

List of Abbrevations

DC	Dioptres cylinder
DS	Dioptres sphere
$ETCO_2$	End-tidal carbon dioxide (% of atmospheric pressure)
FeO_2	Fractional expired oxygen (% of atmospheric pressure)
logMAR	Logarithm of the minimum angle of resolution
Pa	Arterial pressure
$PaCO_2$	Partial pressure of arterial carbon dioxide (mmHg)
PaO_2	Partial pressure of arterial oxygen (mmHg)
pCO_2	Partial pressure of carbon dioxide
PEEP	Positive End-Expiratory Pressure
$PetCO_2$	Partial pressure of end-tidal carbon dioxide (mmHg)
$PetO_2$	Partial pressure of end-tidal oxygen (mmHg)
pO_2	Partial pressure of oxygen

Bibliography

1. Harris A, Jonescu-Cuypers CP, Kagemann L, Ciulla TA, Krieglstein GK. *Atlas of Ocular Blood Flow: Vascular Anatomy, Pathophysiology, and Metabolism*. Philadelphia: Butterworth-Heinemann, 2003.

2. Wolff E. *Eugene Wolff's Anatomy of the Eye and Orbit: Including the central connections, development, and comparative anatomy of the visual apparatus.* 6, revised by R.J. Last ed. Philadelphia: W.B. Saunders Company, 1967.

3. Pournaras CJ, Donati G. In: Albert DM, Jakobiec FA, eds. *Principles and Practice of Ophthalmology*. 2 ed. Philadelphia: W.B. Saunders Co., 2000: 1804-19.

4. Bhutto IA, Lutty GA. In: Shepro D, ed. *Microvascular Research*. Boston: Elsevier Academic Press, 2006: 369-74.

5. Reamington LA. In: *Clinical Anatomy of the Visual System*. Boston: Butterworth-Heineman, 1998: 49-77.

6. Sander B, Larsen M, Moldow B, Lund-Andersen H. Diabetic macular edema: passive and active transport of fluorescein through the blood-retina barrier. *Invest Ophthalmol Vis.Sci.* 2001;**42**:433-8.

7. Sander B, Best J, Johansen S, Kessel L, Moldow B. Fluorescein transport through the blood-aqueous and blood-retinal barriers in diabetic macular edema. *Curr.Eye Res.* 2003;**27**:247-52.

8. Glasgow BJ. Evidence for breaches of the retinal vasculature in acquired immune deficiency syndrome angiopathy. A fluorescent microsphere study. *Ophthalmology.* 1997;**104**:753-60.

9. Lovasik JV, Kergoat H. Consequences of an increase in the ocular perfusion pressure on the pulsatile ocular blood flow. *Optom.Vis.Sci.* 2004;**81**:692-8.

10. Lovasik JV, Kergoat H, Riva CE, Petrig BL, Geiser M. Choroidal blood flow during exercise-induced changes in the ocular perfusion pressure. *Invest Ophthalmol Vis.Sci.* 2003;**44**:2126-32.

11. Riva CE, Titze P, Hero M, Movaffaghy A, Petrig BL. Choroidal blood flow during isometric exercises. *Invest Ophthalmol Vis.Sci.* 1997;**38**:2338-43.

12. Funk RH. Blood supply of the retina. *Ophthalmic Res.* 1997;**29**:320-5.

13. Lu M, Adamis AP. In: Shepro D, ed. *Microvascular Research*. Boston: Elsevier Academic Press, 2006: 401-3.

14. Puro DG. Physiology and pathobiology of the pericyte-containing retinal microvasculature: new developments. *Microcirculation.* 2007;**14**:1-10.

15. Hayreh SS, Zimmerman MB. Fundus changes in central retinal artery occlusion. *Retina.* 2007;**27**:276-89.

16. Flammer J, Orgul S. Optic nerve blood-flow abnormalities in glaucoma. *Prog.Retin.Eye Res.* 1998;**17**:267-89.

17. Fuchsjager-Mayrl G, Wally B, Georgopoulos M, Rainer G, Kircher K, Buehl W et al. Ocular blood flow and systemic blood pressure in patients with primary open-angle glaucoma and ocular hypertension. *Invest Ophthalmol Vis.Sci.* 2004;**45**:834-9.

18. Gilmore ED, Hudson C, Nrusimhadevara RK, Harvey PT, Mandelcorn M, Lam WC et al. Retinal arteriolar diameter, blood velocity, and blood flow response to an isocapnic hyperoxic provocation in early sight-threatening diabetic retinopathy. *Invest Ophthalmol Vis.Sci.* 2007;**48**:1744-50.

19. Gilmore ED, Hudson C, Nrusimhadevara RK, Ridout R, Harvey PT, Mandelcorn M et al. Retinal arteriolar hemodynamic response to an acute hyperglycemic provocation in early and sight-threatening diabetic retinopathy. *Microvasc.Res.* 2007;**73**:191-7.

20. Kifley A, Wang JJ, Cugati S, Wong TY, Mitchell P. Retinal vascular caliber, diabetes, and retinopathy. *Am J Ophthalmol.* 2007;**143**:1024-6.

21. Guan K, Hudson C, Wong T, Kisilevsky M, Nrusimhadevara RK, Lam WC et al. Retinal hemodynamics in early diabetic macular edema. *Diabetes.* 2006;**55**:813-8.

22. Reamington LA. In: *Clinical Anatomy of the Visual System*. Boston: Butterworth-Heinemann, 1998: 177-90.

23. Ishikawa T. Fine structure of retinal vessels in man and the macaque monkey. *Invest Ophthalmol.* 1963;**2:1-15.**:1-15.

24. Sirs JA. The flow of human blood through capillary tubes. *J Physiol.* 1991;**442**:569-83.

25. Nagaoka T, Ishii Y, Takeuchi T, Takahashi A, Sato E, Yoshida A. Relationship between the Parameters of Retinal Circulation Measured by Laser Doppler Velocimetry and a Marker of Early Systemic Atherosclerosis. *Invest.Ophthalmol.Vis.Sci.* 2005;**46**:720-5.

26. Guyton AC, Hall JE. *Textbook of Medical Physiology*. 10th ed. Philadelphia: W.B. Saunders Company, 2000.

27. Kurosaki R, Muramatsu Y, Kato H, Araki T. Protective effect of pitavastatin, a 3-hydroxy-3-methylglutaryl-coenzyme A (HMG-CoA) reductase inhibitor, on ischemia-induced neuronal damage. *Neurol.Res.* 2004;**26**:684-91.

28. Feke GT, Tagawa H, Deupree DM, Goger DG, Sebag J, Weiter JJ. Blood flow in the normal human retina. *Invest Ophthalmol Vis.Sci.* 1989;**30**:58-65.

29. Baer RM, Hill DW. Retinal vessel responses to passive tilting. *Eye.* 1990;**4**:751-6.

30. Liu JH, Gokhale PA, Loving RT, Kripke DF, Weinreb RN. Laboratory assessment of diurnal and nocturnal ocular perfusion pressures in humans. *J Ocul.Pharmacol.Ther.* 2003;**19**:291-7.

31. Feke GT, Pasquale LR. Retinal Blood Flow Response to Posture Change in Glaucoma Patients Compared with Healthy Subjects. *Ophthalmology.* 2007;**115**:246-52.

32. Pournaras CJ. In: Kaiser HJ, Flammer J, Hendrickson P, eds. *Ocular Blood Flow: New Insights into the Pathogenesis of Ocular Diseases*. Basel: Karger, 1995: 40-50.

33. Riva CE, Hero M, Titze P, Petrig B. Autoregulation of human optic nerve head blood flow in response to acute changes in ocular perfusion pressure. *Graefes Arch Clin Exp.Ophthalmol.* 1997;**235**:618-26.

34. Grunwald JE, Sinclair SH, Riva CE. Autoregulation of the retinal circulation in response to decrease of intraocular pressure below normal. *Invest Ophthalmol Vis.Sci.* 1982;**23**:124-7.

35. Robinson F, Riva CE, Grunwald JE, Petrig BL, Sinclair SH. Retinal blood flow autoregulation in response to an acute increase in blood pressure. *Invest Ophthalmol Vis.Sci.* 1986;**27**:722-6.

36. Nemeth J, Knezy K, Tapaszto B, Kovacs R, Harkanyi Z. Different autoregulation response to dynamic exercise in ophthalmic and central retinal arteries: a color Doppler study in healthy subjects. *Graefes Arch Clin Exp.Ophthalmol.* 2002;**240**:835-40.

37. Jeppesen P, Sanye-Hajari J, Bek T. Increased blood pressure induces a diameter response of retinal arterioles that increases with decreasing arteriolar diameter. *Invest Ophthalmol Vis.Sci.* 2007;**48**:328-31.

38. Pose-Reino A, Rodriguez-Fernandez M, Hayik B, Gomez-Ulla F, Carrera-Nouche MJ, Gude-Sampedro F et al. Regression of alterations in retinal microcirculation following treatment for arterial hypertension. *J Clin Hypertens.(Greenwich.).* 2006;**8**:590-5.

39. Jeppesen P, Aalkjaer C, Bek T. Myogenic response in isolated porcine retinal arterioles. *Curr.Eye Res.* 2003;**27**:217-22.

40. Satcher R, Dewey CF, Jr., Hartwig JH. Mechanical remodeling of the endothelial surface and actin cytoskeleton induced by fluid flow. *Microcirculation.* 1997;**4**:439-53.

41. Schmetterer L, Polak K. Role of nitric oxide in the control of ocular blood flow. *Prog.Retin.Eye Res.* 2001;**20**:823-47.

42. Harris A, Ciulla TA, Chung HS, Martin B. Regulation of retinal and optic nerve blood flow. *Arch Ophthalmol.* 1998;**116**:1491-5.

43. Bill A, Sperber GO. Control of retinal and choroidal blood flow. *Eye.* 1990;**4**:319-25.

44. Michelson G, Patzelt A, Harazny J. Flickering light increases retinal blood flow. *Retina.* 2002;**22**:336-43.

45. Polak K, Schmetterer L, Riva CE. Influence of flicker frequency on flicker-induced changes of retinal vessel diameter. *Invest Ophthalmol Vis.Sci.* 2002;**43**:2721-6.

46. Kiryu J, Asrani S, Shahidi M, Mori M, Zeimer R. Local response of the primate retinal microcirculation to increased metabolic demand induced by flicker. *Invest Ophthalmol Vis.Sci.* 1995;**36**:1240-6.

47. Formaz F, Riva CE, Geiser M. Diffuse luminance flicker increases retinal vessel diameter in humans. *Curr.Eye Res.* 1997;**16**:1252-7.

48. Kondo M, Wang L, Bill A. The role of nitric oxide in hyperaemic response to flicker in the retina and optic nerve in cats. *Acta Ophthalmol Scand.* 1997;**75**:232-5.

49. Garhofer G, Huemer KH, Zawinka C, Schmetterer L, Dorner GT. Influence of diffuse luminance flicker on choroidal and optic nerve head blood flow. *Curr.Eye Res.* 2002;**24**:109-13.

50. Linsenmeier RA, Padnick-Silver L. Metabolic dependence of photoreceptors on the choroid in the normal and detached retina. *Invest Ophthalmol Vis.Sci.* 2000;**41**:3117-23.

51. Lovasik JV, Kergoat H, Wajszilber MA. Blue flicker modifies the subfoveal choroidal blood flow in the human eye. *Am J Physiol Heart Circ Physiol.* 2005;**289**:H683-H691.

52. Shakoor A, Blair NP, Mori M, Shahidi M. Chorioretinal vascular oxygen tension changes in response to light flicker. *Invest Ophthalmol Vis.Sci.* 2006;**47**:4962-5.

53. Jean-Louis S, Lovasik JV, Kergoat H. Systemic hyperoxia and retinal vasomotor responses. *Invest Ophthalmol Vis.Sci.* 2005;**46**:1714-20.

54. Eperon G, Johnson M, David NJ. The effect of arterial PO2 on relative retinal blood flow in monkeys. *Invest Ophthalmol.* 1975;**14**:342-52.

55. Gilmore ED, Hudson C, Preiss D, Fisher J. Retinal arteriolar diameter, blood velocity, and blood flow response to an isocapnic hyperoxic provocation. *Am J Physiol Heart Circ Physiol.* 2005;**288**:H2912-H2917.

56. Grunwald JE, Riva CE, Brucker AJ, Sinclair SH, Petrig BL. Altered retinal vascular response to 100% oxygen breathing in diabetes mellitus. *Ophthalmology.* 1984;**91**:1447-52.

57. Dallinger S, Dorner GT, Wenzel R, Graselli U, Findl O, Eichler HG et al. Endothelin-1 contributes to hyperoxia-induced vasoconstriction in the human retina. *Invest Ophthalmol Vis.Sci.* 2000;**41**:864-9.

58. Takagi C, King GL, Takagi H, Lin YW, Clermont AC, Bursell SE. Endothelin-1 action via endothelin receptors is a primary mechanism modulating retinal circulatory response to hyperoxia. *Invest Ophthalmol Vis.Sci.* 1996;**37**:2099-109.

59. Dollery CT, Bulpitt CJ, Kohner EM. Oxygen supply to the retina from the retinal and choroidal circulations at normal and increased arterial oxygen tensions. *Invest Ophthalmol.* 1969;**8**:588-94.

60. Bertuglia S, Giusti A. Role of nitric oxide in capillary perfusion and oxygen delivery regulation during systemic hypoxia. *Am J Physiol Heart Circ Physiol* 2005;**288**:H525-H531.

61. Cabrales P, Tsai AG, Intaglietta M. Nitric oxide regulation of microvascular oxygen exchange during hypoxia and hyperoxia. *J Appl Physiol* 2005; **100**:1181-7.

62. Shibata M, Ichioka S, Kamiya A. Nitric oxide modulates oxygen consumption by arteriolar walls in rat skeletal muscle. *Am J Physiol Heart Circ Physiol* 2005;**289**:H2673-H2679.

63. Iscoe S, Fisher JA. Hyperoxia-induced hypocapnia: an underappreciated risk. *Chest.* 2005;**128**:430-3.

64. Beatty S, Koh H, Phil M, Henson D, Boulton M. The role of oxidative stress in the pathogenesis of age-related macular degeneration. *Surv.Ophthalmol.* 2000;**45**:115-34.

65. Sola A, Rogido MR, Deulofeut R. Oxygen as a neonatal health hazard: call for detente in clinical practice. *Acta Paediatr.* 2007;**96**:801-12.

66. Dorner GT, Garhoefer G, Zawinka C, Kiss B, Schmetterer L. Response of retinal blood flow to CO2-breathing in humans. *Eur J Ophthalmol.* 2002;**12**:459-66.

67. Roff EJ, Harris A, Chung HS, Hosking SL, Morrison AM, Halter PJ et al. Comprehensive assessment of retinal, choroidal and retrobulbar haemodynamics during blood gas perturbation. *Graefes Arch Clin Exp.Ophthalmol.* 1999;**237**:984-90.

68. Venkataraman ST, Hudson C, Fisher JA, Flanagan JG. The impact of hypercapnia on retinal capillary blood flow assessed by scanning laser Doppler flowmetry. *Microvasc.Res.* 2005;**69**:149-55.

69. Wang L, Kondo M, Bill A. Glucose metabolism in cat outer retina. Effects of light and hyperoxia. *Invest Ophthalmol Vis.Sci.* 1997;**38**:48-55.

70. Pakola SJ, Grunwald JE. Effects of oxygen and carbon dioxide on human retinal circulation. *Invest Ophthalmol Vis.Sci.* 1993;**34**:2866-70.

71. Hakim TS, Sugimori K, Camporesi EM, Anderson G. Half-life of nitric oxide in aqueous solutions with and without haemoglobin. *Physiol Meas.* 1996;**17**:267-77.

72. Dorner GT, Garhofer G, Kiss B, Polska E, Polak K, Riva CE et al. Nitric oxide regulates retinal vascular tone in humans. *Am J Physiol Heart Circ Physiol.* 2003;**285**:H631-H636.

73. Buerk DG, Riva CE, Cranstoun SD. Nitric oxide has a vasodilatory role in cat optic nerve head during flicker stimuli. *Microvasc.Res.* 1996;**52**:13-26.

74. Buerk DG, Riva CE, Cranstoun SD. Frequency and luminance-dependent blood flow and K+ ion changes during flicker stimuli in cat optic nerve head. *Invest Ophthalmol Vis.Sci.* 1995;**36**:2216-27.

75. Riva CE, Mendel M, Petrig BL. In: Kaiser HJ, Flammer J, Hendrickson P, eds. *Ocular Blood Flow: New insights into the pathogenesis of ocular diseases.* Basel: Karger, 1996: 128-37.

76. Brunner H, Cockcroft JR, Deanfield J, Donald A, Ferrannini E, Halcox J et al. Endothelial function and dysfunction. Part II: Association with cardiovascular risk factors and diseases. A

statement by the Working Group on Endothelins and Endothelial Factors of the European Society of Hypertension. *J.Hypertens.* 2005;**23**:233-46.

77. Harris A, Kagemann L, Cioffi GA. Assessment of human ocular hemodynamics. *Surv.Ophthalmol.* 1998;**42**:509-33.

78. Zion IB, Harris A, Siesky B, Shulman S, McCranor L, Garzozi HJ. Pulsatile ocular blood flow: relationship with flow velocities in vessels supplying the retina and choroid. *Br J Ophthalmol.* 2007;**91**:882-4.

79. Schmetterer L, Dallinger S, Findl O, Graselli U, Eichler HG, Wolzt M. A comparison between laser interferometric measurement of fundus pulsation and pneumotonometric measurement of pulsatile ocular blood flow. 2. Effects of changes in pCO2 and pO2 and of isoproterenol. *Eye.* 2000;**14**:46-52.

80. Gunvant P, Watkins RJ, Broadway DC, O'Leary DJ. Repeatability and effects of sequential measurements with POBF tonograph. *Optom.Vis.Sci.* 2004;**81**:794-9.

81. Schmetterer L, Dallinger S, Findl O, Eichler HG, Wolzt M. A comparison between laser interferometric measurement of fundus pulsation and pneumotonometric measurement of pulsatile ocular blood flow. 1. Baseline considerations. *Eye.* 2000;**14**:39-45.

82. Polska E, Luksch A, Ehrlich P, Sieder A, Schmetterer L. Measurements in the peripheral retina using LDF and laser interferometry are mainly influenced by the choroidal circulation. *Curr.Eye Res.* 2002;**24**:318-23.

83. Rechtman E, Harris A, Kumar R, Cantor LB, Ventrapragada S, Desai M et al. An update on retinal circulation assessment technologies. *Curr.Eye Res.* 2003;**27**:329-43.

84. Novotny HR, Alvis DL. A method of photographing fluorescence in circulating blood in the human retina. *Circulation.* 1961;**24**:82-6.

85. Winkelman JZ, Zappia RJ, Gay AJ. Human arm to retina circulation time. Determination by simultaneous fluorophotometry. *Arch Ophthalmol.* 1971;**86**:626-36.

86. Feke GT, Riva CE. Laser Doppler measurements of blood velocity in human retinal vessels. *J Opt.Soc.Am.* 1978;**68**:526-31.

87. Riva CE, Feke GT, Eberli B, Benary V. Bidirectional LDV system for absolute measurement of blood speed in retinal vessels. *Applied Optics* 1979;**18**:2301-6.

88. Riva CE, Grunwald JE, Sinclair SH, O'Keefe K. Fundus camera based retinal LDV. *Applied Optics* 1980;**20**:117-20.

89. Guan K, Hudson C, Flanagan JG. Variability and repeatability of retinal blood flow measurements using the Canon Laser Blood Flowmeter. *Microvasc.Res.* 2003;**65**:145-51.

90. Yoshida A, Feke GT, Mori F, Nagaoka T, Fujio N, Ogasawara H et al. Reproducibility and clinical application of a newly developed stabilized retinal laser Doppler instrument. *Am J Ophthalmol.* 2003;**135**:356-61.

91. Azizi B, Buehler H, Venkataraman ST, Hudson C. Impact of simulated light scatter on the quantitative, noninvasive assessment of retinal arteriolar hemodynamics. *J Biomed.Opt.* 2007;**12**:034021.

92. Michelson G, Schmauss B, Langhans MJ, Harazny J, Groh MJ. Principle, validity, and reliability of scanning laser Doppler flowmetry. *J Glaucoma.* 1996;**5**:99-105.

93. Riva CE, Grunwald JE, Sinclair SH. Laser Doppler Velocimetry study of the effect of pure oxygen breathing on retinal blood flow. *Invest Ophthalmol.Vis.Sci.* 1983;**24**:47-51.

94. Hague S, Hill DW, Crabtree A. The calibre changes of retinal vessels subject to prolonged hyperoxia. *Exp.Eye Res.* 1988;**47**:87-96.

95. Sponsel WE, DePaul KL, Zetlan SR. Retinal hemodynamic effects of carbon dioxide, hyperoxia, and mild hypoxia. *Invest Ophthalmol Vis.Sci.* 1992;**33**:1864-9.

96. Schmetterer L, Lexer F, Findl O, Graselli U, Eichler HG, Wolzt M. The effect of inhalation of different mixtures of O2 and CO2 on ocular fundus pulsations. *Exp.Eye Res.* 1996;**63**:351-5.

97. Chung HS, Harris A, Halter PJ, Kagemann L, Roff EJ, Garzozi HJ et al. Regional differences in retinal vascular reactivity. *Invest Ophthalmol.Vis.Sci.* 1999;**40**:2448-53.

98. Strenn K, Menapace R, Rainer G, Findl O, Wolzt M, Schmetterer L. Reproducibility and sensitivity of scanning laser Doppler flowmetry during graded changes in PO2. *Br.J.Ophthalmol.* 1997;**81**:360-4.

99. Kiss B, Polska E, Dorner G, Polak K, Findl O, Mayrl GF et al. Retinal blood flow during hyperoxia in humans revisited: concerted results using different measurement techniques. *Microvasc.Res.* 2002;**64**:75-85.

100. Luksch A, Garhofer G, Imhof A, Polak K, Polska E, Dorner GT et al. Effect of inhalation of different mixtures of O(2) and CO(2) on retinal blood flow. *Br.J.Ophthalmol.* 2002;**86**:1143-7.

101. Vucetic M, Jensen PK, Jansen EC. Diameter variations of retinal blood vessels during and after treatment with hyperbaric oxygen. *Br J Ophthalmol.* 2004;**88**:771-5.

102. Gilmore ED, Hudson C, Venkataraman ST, Preiss D, Fisher J. Comparison of different hyperoxic paradigms to induce vasoconstriction: implications for the investigation of retinal vascular reactivity. *Invest Ophthalmol Vis.Sci.* 2004;**45**:3207-12.

103. Harris A, Kagemann L, Ehrlich R, Rospigliosi C, Moore D, Siesky B. Measuring and interpreting ocular blood flow and metabolism in glaucoma. *Can.J.Ophthalmol.* 2008;**43**:1-9.

104. Jensen FB. Red blood cell pH, the Bohr effect, and other oxygenation-linked phenomena in blood O2 and CO2 transport. *Acta Physiol Scand.* 2004;**182**:215-27.

105. Becker H, Polo O, McNamara SG, Berthon-Jones M, Sullivan CE. Ventilatory response to isocapnic hyperoxia. *J Appl Physiol.* 1995;**78**:696-701.

106. Becker HF, Polo O, McNamara SG, Berthon-Jones M, Sullivan CE. Effect of different levels of hyperoxia on breathing in healthy subjects. *J Appl Physiol.* 1996;**81**:1683-90.

107. Mulkey DK, Henderson RA, III, Putnam RW, Dean JB. Hyperbaric oxygen and chemical oxidants stimulate CO2/H+-sensitive neurons in rat brain stem slices. *J Appl Physiol.* 2003;**95**:910-21.

108. Dautrebande L, Haldane JS. The effects of respiration of oxygen on breathing and circulation. *J Physiol.* 1921;**55**:296-9.

109. Kergoat H, Faucher C. Effects of oxygen and carbogen breathing on choroidal hemodynamics in humans. *Invest Ophthalmol Vis.Sci.* 1999;**40**:2906-11.

110. Rose PA, Hudson C. Comparison of retinal arteriolar and venular variability in healthy subjects. *Microvasc.Res.* 2007;**73**:35-8.

111. Hosking SL, Harris A, Chung HS, Jonescu-Cuypers CP, Kagemann L, Roff Hilton EJ et al. Ocular haemodynamic responses to induced hypercapnia and hyperoxia in glaucoma. *Br.J.Ophthalmol.* 2004;**88**:406-11.

112. Lindholm P, Karlsson L, Gill H, Wigertz O, Linnarsson D. Time components of circulatory transport from the lungs to a peripheral artery in humans. *Eur.J.Appl.Physiol.* 2006;**97**:96-102.

113. Rose PA, Schnitzer A, Hudson C. Effect of Caffeine on Retinal Arteriolar Vascular Reactivity in Young, Normal Subjects. *FASEB J.* 2006;**20**:A286-A28b.

114. Langhans M, Michelson G, Groh MJ. Effect of breathing 100% oxygen on retinal and optic nerve head capillary blood flow in smokers and non-smokers. *Br J Ophthalmol.* 1997;**81**:365-9.

115. Hazel CA, Elliott DB. The dependency of logMAR visual acuity measurements on chart design and scoring rule. *Optom.Vis.Sci.* 2002;**79**:788-92.

116. Slessarev M, Fisher JA Volgyesi G Prisman E Mikulis D Hudson C Ansel C. A new method and apparatus to attain and maintain target end tidal gas concentrations. PCT/CA2005/001166(WO/2007/012170). 1-2-2007.
Ref Type: Patent

117. Harris A, Jonescu-Cuypers CP, Kagemann L, Ciulla TA, Krieglstein GK. In: *Atlas of Ocular Blood Flow*. Philadelphia: Butterworth-Heinemann, 2003: 19-70.

118. Guyton AC, Hall JE. In: *Textbook of Medical Physiology*. 10th ed. Philadelphia: W.B. Saunders Company, 2000: 452-62.

119. Banzett RB, Garcia RT, Moosavi SH. Simple contrivance "clamps" end-tidal PCO(2) and PO(2) despite rapid changes in ventilation. *J Appl Physiol.* 2000;**88**:1597-600.

120. Venkataraman ST, Hudson C, Fisher JA, Flanagan JG. Novel methodology to comprehensively assess retinal arteriolar vascular reactivity to hypercapnia. *Microvasc.Res.* 2006;**72**:101-7.

121. Yu DY, Cringle SJ, Yu PK, Su EN. Intraretinal oxygen distribution and consumption during retinal artery occlusion and graded hyperoxic ventilation in the rat. *Invest Ophthalmol Vis.Sci.* 2007;**48**:2290-6.

122. Cringle SJ, Yu DY, Yu PK, Su EN. Intraretinal oxygen consumption in the rat in vivo. *Invest Ophthalmol Vis.Sci.* 2002;**43**:1922-7.

123. Yu DY, Cringle SJ. Oxygen distribution in the mouse retina. *Invest Ophthalmol Vis.Sci.* 2006;**47**:1109-12.

124. Cringle SJ, Yu DY. Intraretinal oxygenation and oxygen consumption in the rabbit during systemic hyperoxia. *Invest Ophthalmol Vis.Sci.* 2004;**45**:3223-8.

125. Braun RD, Linsenmeier RA, Goldstick TK. Oxygen consumption in the inner and outer retina of the cat. *Invest Ophthalmol Vis.Sci.* 1995;**36**:542-54.

126. Cringle SJ, Yu DY. A multi-layer model of retinal oxygen supply and consumption helps explain the muted rise in inner retinal PO(2) during systemic hyperoxia. *Comp Biochem.Physiol A Mol.Integr.Physiol.* 2002;**132**:61-6.

127. Riva CE, Cranstoun SD, Grunwald JE, Petrig BL. Choroidal blood flow in the foveal region of the human ocular fundus. *Invest Ophthalmol Vis.Sci.* 1994;**35**:4273-81.

128. Geiser MH, Riva CE, Dorner GT, Diermann U, Luksch A, Schmetterer L. Response of choroidal blood flow in the foveal region to hyperoxia and hyperoxia-hypercapnia. *Curr.Eye Res.* 2000;**21**:669-76.

129. Riva CE, Pournaras CJ, Tsacopoulos M. Regulation of local oxygen tension and blood flow in the inner retina during hyperoxia. *J Appl Physiol.* 1986;**61**:592-8.

130. Landers MB, III. Retinal oxygenation via the choroidal circulation. *Trans.Am Ophthalmol Soc.* 1978;**76:528-56.**:528-56.

131. Ashton N, Ward B, Serpell G. Role of oxygen in the genesis of retrolental fibroplasia; a preliminary report. *Br J Ophthalmol.* 1953;**37**:513-20.

132. Slessarev, M. Response of cerebral blood flow to square wave changes in PetCO2 and PetO2 in spontaneously breathing humans. 2006. Department of Physiology, University of Toronto.
Ref Type: Thesis/Dissertation

133. Tayyari, F. The Relationship Between Retinal Vascular Reactivity and Arteriolar Diameter. 2006. University of Waterloo.
Ref Type: Thesis/Dissertation

134. Parker JD, Thiessen JJ, Reilly R, Tong JH, Stewart DJ, Pandey AS. Human endothelin-1 clearance kinetics revealed by a radiotracer technique. *J.Pharmacol.Exp.Ther.* 1999;**289**:261-5.